The Hydrologic and Geomorphic Impacts of the 2010 Fourmile Canyon Fire, Boulder Creek Watershed, CO

by

Benjamin Purinton
Class of 2013

A thesis submitted to the
faculty of Wesleyan University
in partial fulfillment of the requirements for the
Degree of Bachelor of Arts
with Departmental Honors in Earth & Environmental Sciences

Acknowledgements

Contents

Figures

Tables

Abstract

A September 2010 large wildfire burned 23% of Fourmile Canyon, a high relief, high gradient tributary basin to the Boulder Creek watershed west of Boulder, Colorado. Cover loss through the combustion of litter and vegetation combined with heat-induced soil hydrophobicity produced extreme runoff events including a 70-year flood in Fourmile Creek. This and other floods resulted from high frequency rain events with return periods of 1–5 years. Hydrographic and rainfall analysis display significant changes in postfire hydrology including hydrograph shape and rainfall-runoff response, along with rapid recovery in peak flows since the fire. Sediment yield increased through erosion on burned hillslopes, delivering approximately 39,400 t of sediment over the past two years. Field evidence and stream hydrology suggests that the return of vegetation and rewetting of hydrophobic soils may quickly reduce hillslope runoff and erosion. Activities of ^{137}Cs and ^{210}Pb are higher in hillslope ash than O and A soil horizons on unburned slopes. The ash radionuclide and geochemical signature, in the form of major oxides formed during the combustion of organic matter, is measured in fresh overbank deposits from the valley floor of Fourmile Canyon. The ash signature in these deposits is also found in grain-size results. Geochemical analysis of trace metals in overbank deposits document the effect of historical mining in Fourmile Canyon. Channel storage increases sediment residence time in the watershed, as reduced peak flows will limit the stream's ability to transport sediment. The increased hillslope erosion and sediment deposition along Fourmile Creek caused by the wildfire may be a primary contributor to geomorphic change in similar fire-prone landscapes. Using estimates of fire-flood recurrence, long-term denudation rates extrapolated from estimated sediment yield fall within a range of 4–90 m/Myr of long-term erosion dependent on burned area considered, hillslope recovery, and return periods of fire and rain.

1. <u>Introduction</u>

Wildfire is essential to stand succession in mountainous fire-prone regions (MacDonald and Stednick, 2003). From 1980 to 2011, 48 fires burned a total of 242,500 acres in the Colorado Front Range alone, with 13 fires accounting for 85% of this acreage (Graham *et al.*, 2012). Frequent small fires have limited impact on ecology, chemistry, hydrology, and geomorphology. However, recent trends indicate that the frequency of severe fires capable of drastically altering the landscape appears to be increasing, possibly in relation to climate change (Saunders *et al.*, 2008).

By removing vegetation and altering soil properties, wildfire dramatically changes the hydrologic regime and movement of sediment in watersheds. Steep, fire-prone terrains, such as those found in the Colorado Front Range, are especially susceptible to these effects. Over long time scales, repeated severe fires are capable of significant geomorphic change (Swanson, 1981). Disturbance caused by fire has the small-scale effect of decreasing infiltration and increasing runoff on hillslopes and the large-scale effect of increasing sediment yield and peak flows in channel networks (Shakesby and Doerr, 2006). Wildfire also effects water quality through nutrient loading and increasing suspended sediment and turbidity (Smith *et al.*, 2011a).

Understanding the hydrologic and erosional response of catchments to wildfire can lead to better damage mitigation techniques and assessment of long-term impacts. Such studies are of great importance where other human activity, like mining, can contribute to these detrimental impacts. The 2010 Fourmile Canyon Fire, which burned 23% of the Fourmile Creek drainage, provides a unique opportunity of

studying the effects of severe wildfire at the urban-wilderness interface near Boulder, CO.

1.1. Burn Severity and Fire Frequency

Immediately following wildfire, remote sensing is used to quantify the area exposed by the combustion of vegetation, referred to as burn severity (Moody, 2011). Burn severity serves as a proxy for the potential hydrologic and geomorphic effects in a given location. Low severity burning is typified by little or no consumption of litter and no change to the mineral soil. In moderate severity burns, some consumption of litter and duff occurs. High severity burns experience the largest impact as soils are heated to high temperatures at depth and near complete combustion of duff, litter, and vegetation occurs (Ice *et al.*, 2004).

The recurrence interval of severe, stand-replacing fires in the low elevation, xeric, mixed ponderosa pine and Douglas fir forests of the Front Range has been estimated at 50–60 years for a given location (Kaufmann *et al.*, 2000). Other estimates for fire recurrence in the Rocky Mountains range from 30–100 years (Elliot and Parker, 2001; Meyer and Pierce, 2003; Sherriff and Veblen, 2007). Since the mid-1980s the frequency of fire in the Western United States has increased four-fold, over six times as much area is now burned per year, and the duration of the fire season has increased by 78 days (Westerling *et al.*, 2006). These changes are likely tied to anthropogenic climate change, and may lead to continually increased severe wildfire frequency in the future.

1.2. Wildfire Effects and Recovery

The physical effects of wildfire on basin hydrology and erosional processes can be divided into (1) the development of soil water repellency in severely burned topsoil, (2) the deposition of a wettable ash layer on the soil surface, and (3) cover loss through the combustion of vegetation and ground litter (Wondzell and King, 2003; Shakesby and Doerr, 2006).

As defined by Moody and Martin (2001a) relaxation time following disturbance–wildfire–is the length of time between an initial phase where process rates increase to some maximum and the recovery phase where these process rates decrease to their pre-disturbance static values (Fig. 1.1). Fire acts to quickly increase sediment yield to a peak followed by prolonged return to background yield with the return of vegetation and litter cover and removal of readily erodible fines. The same is true of rainfall-runoff relations, as increased percentage of rainfall converted to runoff fades rapidly with revegetation (Soto *et al.*, 1993).

Significantly elevated sediment delivery and peak discharges typically last up to two years, making catchments vulnerable to catastrophic flooding and erosion soon after wildfire (Kunze and Stednick, 2006; Wilkinson *et al.*, 2009). This initial 1–2 year disturbance is followed by elevated hydrological and erosional effects persisting for about 3–10 years, mostly dependent on the time required for revegetation (Moody and Martin, 2001a; Benavides-Solorio and MacDonald, 2005; Shakesby and Doerr, 2006). While hillslopes recover rapidly following wildfire, channels recover on longer decadal time scales due to the large sediment influx (Legleiter *et al.*, 2003).
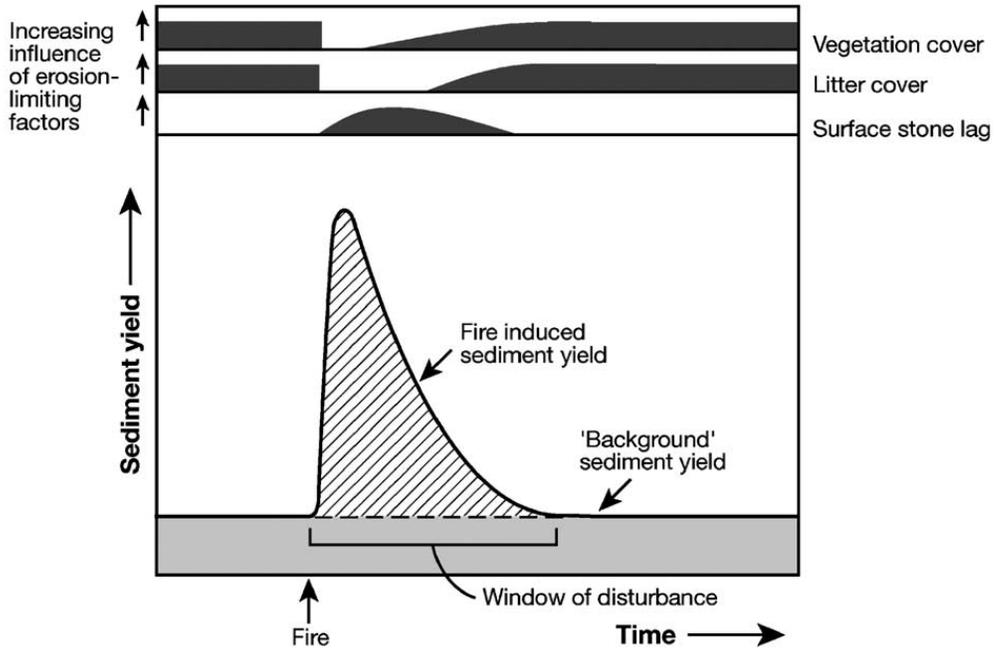
Figure 1.1. Idealized rapid increase in sediment yield against background following wildfire. The "window of disturbance" represents prolonged recovery by return of cover and depletion of readily available fine material (stone lag). Modified from Swanson (1981) (Shakesby and Doerr, 2006).

1.3. Hydrologic Response

The hydrologic effects of wildfire result in decreased infiltration of rainfall and increased runoff (Ice *et al.*, 2004). In steep, severely burned basins this response is evident in short-duration, high intensity, low volume rainfall events of short recurrence intervals generating floods with long recurrence intervals (Shakesby and Doerr, 2006). Spring snowmelt discharge may occur earlier due to loss of tree shade and the reduced albedo of soot covered snowpack, although there has been limited research into these effects (Shakesby and Doerr, 2006).

The initial cause of increased discharge is the generation of a two-layer system consisting of water repellent mineral soil overlain by fine, wettable ash (Fig. 1.2). Combusted hydrophobic organic compounds from the O- and upper A-horizons of soils condense in deeper, cooler underlying mineral soil, insulated from the heat of

4

the fire (DeBano, 2000). This hydrophobic layer exists naturally in unburned O-horizons; however, the concentrating effect of fire enhances its water repellency (Huffman *et al.*, 2001). Hydrophobicity usually appears in the top ~5 cm of mineral soil, with increasing burn severity increasing its repellency and thickness (Certini, 2005).

The ash layer is made up of soot, charcoal, charred material, and mineral material ranging in thickness from less than a centimeter to 10s of centimeters (Moody *et al.*, 2009; Smith *et al.*, 2011a). This wettable ash is capable of holding half or more of its thickness in water (Bookter, 2006; Cerdà and Doerr, 2008; Stoof *et al.*, 2010). The presence of ash creates a complex hydrological response during the first rain events after wildfire.
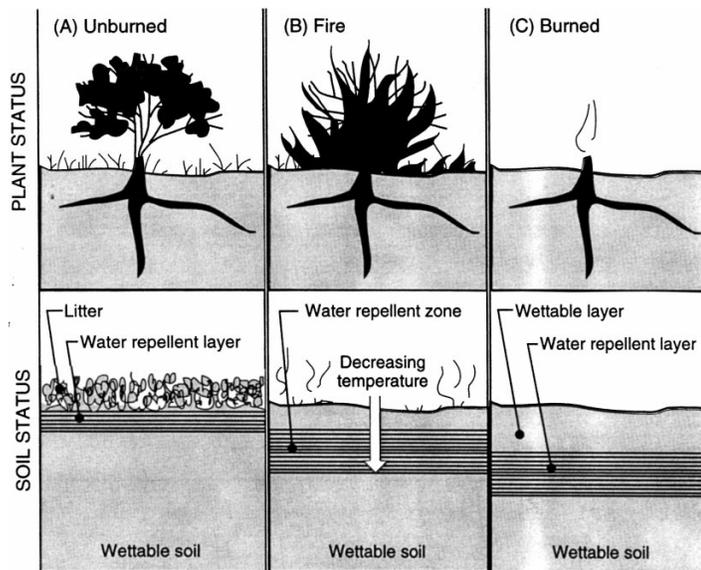
Figure 1.2. Two layer system generated by wildfire. Ash depicted as "wettable layer" overlying hydrophobic "water repellent layer". Also note cover loss of plants and litter (DeBano, 2000).

Initially only rain volumes capable of saturating the absorbent ash generate runoff, as the rain cannot infiltrate into the hydrophobic mineral soil (Woods and Balfour, 2010). Sufficient saturation can increase shear stress and cause failure of the

5

ash layer (Gabet and Bookter, 2011). Rain directly on exposed hydrophobic mineral

soil causes runoff by Hortonian overland flow (Fig. 1.3). Uncovered, water repellent

soils have low infiltration rates capable of contributing up to 80% of rainfall to

overland flow (Moody and Martin, 2001a; Onda *et al.*, 2008). Because the ash is

stripped within 1–2 years of the fire (Reneau *et al.*, 2007) and soil water repellency

persists for only months (Huffman *et al.*, 2001; Moody and Ebel, 2012), other effects

of wildfire are also responsible for elevated runoff and discharge in the 3–10 year

disturbance widow.
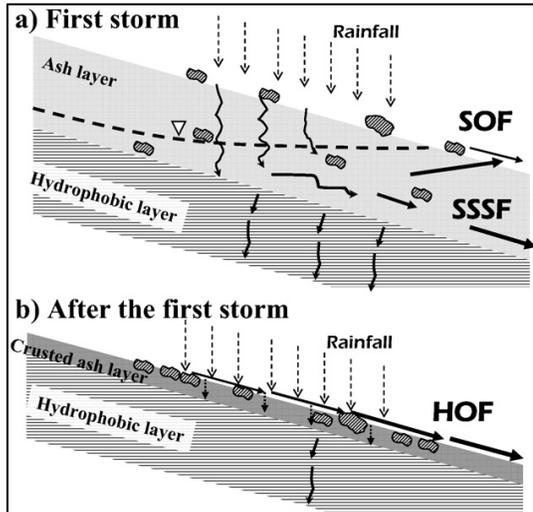
Figure 1.3. a) Initial response limited by presence of wettable ash causing subsurface storm flow (SSSF) and saturation overland flow (SOF) with sufficient rain volume. b) Response to additional rainfall after removal of ash. Rain with intensity greater than infiltration rate of hydrophobic layer generates Hortonian overland flow (HOF). Also note "crusted ash layer" contributing to surface sealing (Onda *et al.*, 2008).

The reduced aggregate stability of heated soil particles allows easy

detachment by rain splash (Kunze and Stednick, 2006). Detached soil and ash

particles clog macropores in the upper mineral soil creating a surface seal (Fig. 1.3b)

leading to increased runoff (Parise and Cannon, 2012). With a median grain size of

59 ± 10 μm, ponderosa pine ash easily fills pore spaces in coarse soils, contributing to

surface sealing (Bookter, 2006).

Cover loss is the chief culprit in generating elevated discharge in the years following wildfire. By decreasing interception and evapotranspiration and creating a smooth, obstacle free surface, wildfires construct low energy pathways for runoff (Larsen *et al.*, 2009). Rapid returns of grasses, shrubs, and plant litter are responsible for the small disturbance window associated with even the largest fires.

Short summertime convective storms in the Front Range release the majority of rain within their first 30 minutes (Moody and Martin, 2001b). Therefore, wildfire studies in this region use maximum 30-minute rainfall intensity (I_{30}) to quantify differences in runoff response (e.g. Moody *et al.*, 2008; Kunze and Stednick, 2006). A threshold I_{30}=10–20 mm/hr is often cited for significant runoff immediately following wildfire (Cannon *et al.*, 2001, MacDonald and Stednick, 2003; Kunze and Stednick, 2006). Though, this value fluctuates with the spatial variation of burn severity and rainfall on slopes of varying gradients (Ryan *et al.*, 2011).

1.4. Sediment Erosion and Transport

The hydrological impacts of wildfire generate significantly elevated sediment yields. The initial rain-on-burn erosive effect can be seen in the stripping of ash soon after wildfire (Reneau *et al.*, 2007). As pore pressure increases with additional rain, intergranular stress decreases, shear stress drops, and the ash layer is able to cascade downslope by sheetwash and rilling (Fig. 1.4). Raindrop impact on dry, non-cohesive soils can entrain additional fine particles in this water-soil mass, causing a rise in shear stress that allows entrainment of larger particles (DeBano, 2000; Gabet and Sternberg, 2008).

(A)
Wettable layer
Increasing pore pressure
Water repellent layer
Underlying wettable soil

(D)
Free-flowing water
Water repellent layer
Underlying wettable soil

(B)
Failure Zone
Water repellent layer

(E)
Free-flowing water
Underlying wettable soil

(C)
Free-flowing water
Water repellent layer

(F)
RILL
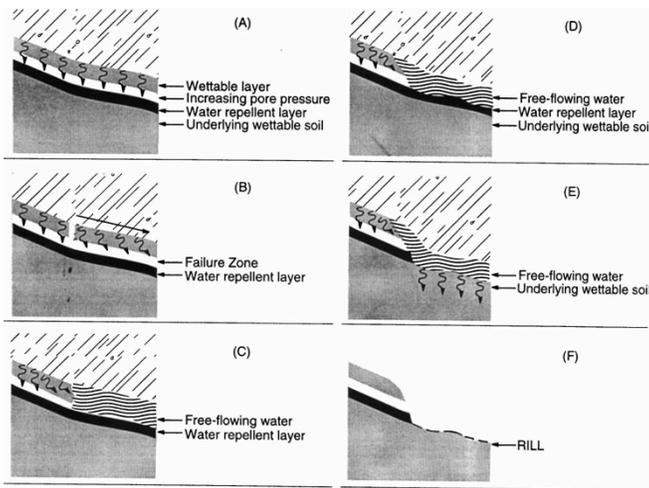
Figure 1.4. Failure of saturated ash layer through excessive rainfall depicted in panels (A)–(C). (D), Generation of overland flow above water repellent layer. (E), Stripping of water repellent layer with additional rainfall (DeBano, 2000).

As shear stress rises to a critical point through the progressive addition of sediment in runoff, debris flows are created (Meyer and Wells, 1997; Parise and Cannon, 2012). Readily erodible fine ash material is an essential component in the creation of these destructive slurries (Gabet and Sternberg, 2008). Debris flows in the Front Range can be generated by rain events with 1–2 year recurrence intervals immediately following wildfire (Cannon *et al.*, 2008). Convective rainstorms with $I_{30} \geq 10$ mm/hr generate about 80% of postfire erosion, primarily through entrainment of sediment in overland flow (MacDonald and Stednick, 2003).

Benavides-Solorio and MacDonald (2005) determined that 90% of postfire sediment delivery was accomplished by summer convective storms for three wildfires (Bobcat, Bear Tracks, and Hourglass) and three prescribed fires (Dadd Bennett, Lower Flowers, and Crosier Mountain) throughout the Front Range. This was at a rate of 0.2–1 kg/m^2/y on high-severity burned slopes, but only 0.005 and 0.02 kg/m^2/y on low and moderately burned slopes respectively. Percentage bare soil, analogous to burn severity, is an indicator of potential sediment yield. Larsen *et al.* (2009) determined consistently high yields where ground cover was less than 40% following

wildfire (Fig. 1.5). Studies describe some postfire sediment yields of 200 times background levels (Moody and Martin, 2001a; Wilkinson *et al.*, 2009).
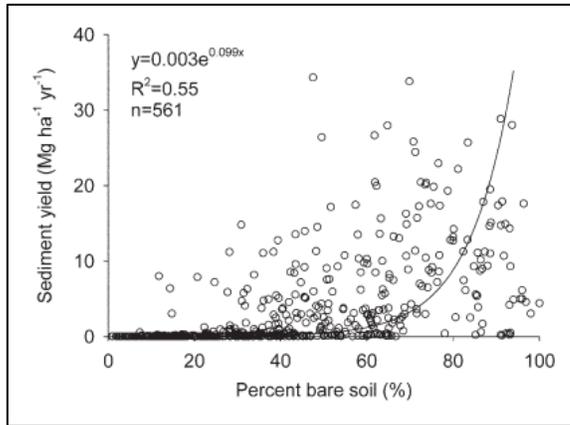
Figure 1.5. Sediment yield associated with increasing percent bare soil. Variability caused by lithology, soil, rainfall, and basin characteristics. Data gathered from 10 studies in the Colorado Front Range with each point representing annual sediment yield from a burned slope (Larsen *et al.*, 2009).

Rainfall events are most effective at generating elevated sediment yields when centered on steep, severely burned slopes (Ryan *et al.*, 2011). Spatial and temporal differences in burning and rainfall lead to a complex response in basin-wide sediment delivery (Moody and Martin, 2001a). Prefire periods represent supply-limited erosional systems in terms of available sediment. But following wildfire these systems become transport-limited, requiring high frequency rainfall events over severely burned areas to transport exposed ash and soil prior to revegetation (Moody and Martin, 2001a; Shakesby and Doerr, 2006, Ryan *et al.*, 2011).

1.5. Long-term Geomorphic Contribution

In the months to years following fire, pulses of surface sediment from charred hillslopes characterize erosion. As erosion declines on these slopes a second period of elevated catchment yield occurs. Sediments deposited on footslopes and floodplains are remobilized by successive flood events, slowly washing out into larger drainages

over decadal scales (Legleiter *et al.*, 2003; Wilkinson *et al.*, 2009). The geomorphic impact of this sediment influx can be a key driver in landscape evolution (Swanson, 1981). Moody and Martin (2001a) found 67% of sediment eroded from burned slopes to be stored in channel floodplains, becoming persistent landscape features with residence times estimated at 300 years.

Long-term (kyr-Myr) erosion rates cannot be reliably determined by short-term erosional studies in undisturbed areas. When compared to long-term rates, short-term erosion rates have been found to be 17 times lower in the Rocky Mountains (Kirchner *et al.*, 2001). It is theorized that the high rate of long-term erosion in these cases is caused by episodic sediment delivery from catastrophic events such as fire, flooding, or the combination of both (Pierce *et al.*, 2004). Demonstrated coupling of fire-flood events (Elliot and Parker, 2001), indicates that increasing fire frequency increases the frequency of these geomorphic events. This effect is pronounced when rare rain events occur shortly after severe wildfire (Moody and Martin, 2001a), but even common rain events are capable of generating significant discharge and sediment input prior to recovery (Cannon *et al.*, 2008; Ryan *et al.*, 2011). The erosional effect of such events has been estimated at 30–97% of sediment delivery in mountainous fire-prone landscapes, dependent on return periods of fire and rainfall (Swanson, 1981; Kirchner *et al.*, 2001; Wilkinson *et al.*, 2009).

1.6. Water and Sediment Chemistry

Additional hydrologic and geomorphic impacts of wildfire are significant changes observed in water and sediment chemistry, with the potential for detrimental downstream impacts. Increased concentrations of C, N, P, Ca^{2+}, Cl^-, K^+, Mg^{2+}, Na^+,

SO_4^{2-} and various trace metals, along with increased pH, are common in water chemistry following wildfire (Chorover *et al.*, 1994; Mast and Clow, 2008; Smith *et al.*, 2011a). These nutrient increases are associated with the combustion and mineralization of organic matter (Rhoades *et al.*, 2011). The increased nutrient loading causes algal blooms, impacting stream ecosystems and water quality (Wilkinson *et al.*, 2009). Turbidity and total suspended sediment also increase through the input of fine ash and mineral soil from hillslopes (Smith *et al.*, 2011a).

The greatest concern to water quality is ash that is stripped from the burned slopes within 1–2 years and readily transported downstream (Reneau *et al.*, 2007). Gabet and Bookter (2011) demonstrated that ponderosa pine ash is primarily composed of Al, Ca, Fe, K, Mg, Mn, and P. Combustion of organic matter reduces organic C and C/N ratios in the soil of burned slopes (Dyrness *et al.*, 1989). Extreme heat leads to the mineralization of organic matter and ash enriched in soluble oxides of alkali metals and cations, such as K^+ and Na^+, causing increased pH in surface soils (Dyrness *et al.*, 1989; Certini, 2005). The accumulation of Mn in organic matter accounts for increased concentrations of Mn in burned soil and ash (Gonzalez Parra *et al.*, 1996; Smith *et al.*, 2012).

1.7. Sediment Source and Tracing

Sediment tracing is of interest in the assessment of long-term landscape change and hillslope/river coupling, as well as short-term impacts on water quality. Research into the determination of sediment sources in a discrete drainage is complex, requiring well-constrained sources and proper models to determine individual inputs to the overall mixture (D'Haen *et al.*, 2012). However, field

observations and knowledge of hydrologic and geomorphic processes can provide insight into the sources of sediment in a small drainage network (Owens *et al.*, 2006).

Perhaps the most promising method of sediment source tracing comes from the use of fallout radionuclides associated with atmospheric nuclear testing. Increases of ^{137}Cs and ^{210}Pb activity in ash deposits derive from combustion of organic matter and litter, where these radioactive elements concentrate (Wilkinson *et al.*, 2009; Smith *et al.*, 2011b). Activity of ^{137}Cs in ash deposits has been measured at 40 times background levels (Johansen *et al.*, 2003).

Reneau *et al.* (2007) tested loamy, charcoal-rich deposits in alluvial stratigraphy associated with a fire in New Mexico. The results indicated (1) the affinity of ^{137}Cs to adhere to fine silts and clays and (2) 90% of hillslope ash was delivered one year after the fire based on rapid declines in ^{137}Cs activity in subsequent depositional stratigraphic layers. As fallout radionuclides adhere to particles in the silt to clay range, their utility in analyzing total sediment output is more limited than analyzing the contribution of fine sediment, primarily ash, to postfire yields (Wilkinson *et al.*, 2009). However, since contaminants also tend to bind on the fine ash material (Plumlee *et al.*, 2007), characterizing its movement is key in determining downstream water quality impacts (Smith *et al.*, 2011a).

Despite sediment tracing limitations, previous research and observation has demonstrated trends in postfire sediment delivery. When intense rainfall is combined with severe burn in steep and narrow catchments with low storage capacity, it is probable that hillslope material will dominate sediment input in the short term (Wilkinson *et al.*, 2009; Smith *et al.*, 2011b). As ash is stripped, soil hydrophobicity

is degraded, and vegetation is reinstated, channels return as the dominant sediment source, with abundant fire-associated sediment along channel banks available for remobilization (Moody and Martin, 2009).

1.8. Study Site

Fourmile Canyon, located just outside Boulder, CO, is a tributary to the upper Boulder Creek basin (Fig. 1.6). The drainage area of Fourmile Creek at the point of a U.S. Geological Survey stream gauge–0.4 km upstream of its confluence with Boulder Creek–is 63 km^2 (USGS StreamStats, 2012; USGS Surface-Water, 2012). The Fourmile Canyon Watershed is generally steep with an average slope of 20°, numerous side slopes approaching or above 45°, and an average channel gradient of 37 m/km (Graham *et al.*, 2012; USGS StreamStats, 2012). The watershed ranges in elevation from 1600 to 2900 m with a mean elevation of 2430 m (Graham *et al.*, 2012). The main tributary of Fourmile Creek, Gold Run, has a drainage area of 7.1 km^2 (USGS StreamStats, 2012).

Mean precipitation in the area is 533 mm/yr, with a significant portion falling as snow in winter months (Murphy *et al.*, 2000). Maximum summer precipitation occurs in July and August associated with monsoonal convective storms (Ebel *et al.*, 2012). Vegetation is aspect controlled with ponderosa pine interspersed with Rocky Mountain Juniper dominating south-facing slopes and aspen, Douglas fir, and Limber Pine dominating north-facing slopes (Ebel *et al.*, 2012).

The upper basin of Fourmile Creek is composed primarily of gneisses and schists (~1.8 Ga) intruded in the lower basin by Boulder Creek Granodiorite (~1.7 Ga) and Silver Plume Granite (~1.4 Ga). Intrusive dikes (~30–60 Ma) containing

metallic ores of gold, silver, tungsten, and copper are common (Murphy *et al.*, 2000; Beganskas, 2012). Boulder Creek Granodiorite is the dominant near surface bedrock in the catchment, with well-drained gravelly sandy loam soils defined as frigid Lamellic and Typic Haplustalf type derived predominantly from the weathering of this source rock (Ebel *et al.*, 2012).
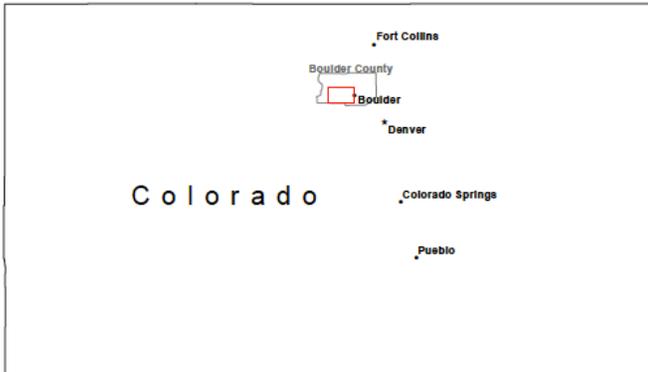
Figure 1.6. Location of Fourmile Creek Watershed within Boulder County, Colorado.
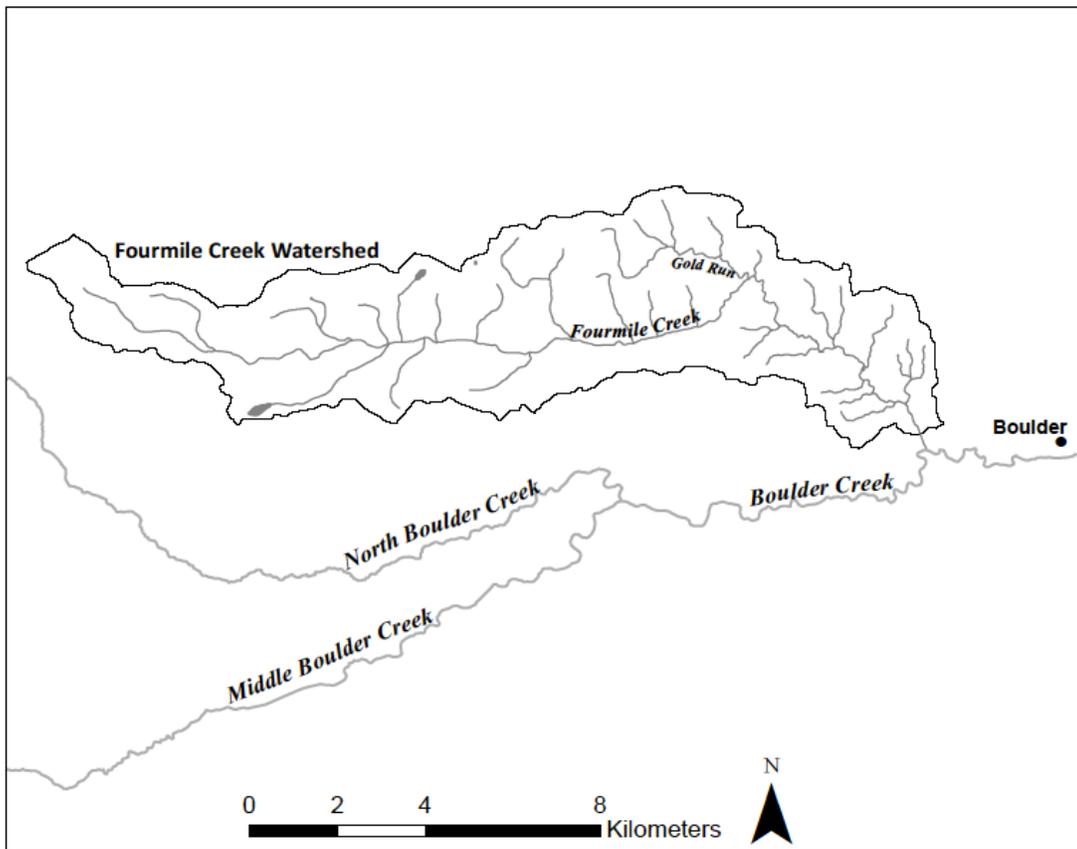
[State, County, Cities: ESRI ArcGIS Online; Hydrography: USGS; Watershed: USGS StreamStats]

1.9. Current Use and Mining History

Much of Fourmile Canyon is presently developed as individual housing lots. Houses are found on either side of the channel along the entire reach of Fourmile Creek, becoming dense in some wider areas of the valley. The north bank of the creek is constrained by Fourmile Drive, providing access over the length of the canyon.

Fourmile was originally settled in 1859 by miners exploiting gold deposits found in the intrusive veins around Gold Hill (Fig. 1.7). The discovery of free and pyritic gold quickly diminished and the area was largely abandoned. However, the discovery of telluride gold ore in 1872 allowed the industry to continue into the early 1900s (Twitty, 2007). An abandoned railroad grade associated with the canyon's early settlement constrains Fourmile Creek along much of its south bank.

Mining in Fourmile Canyon causes high Au concentrations in streambed and floodplain sediments (D. Dethier, personal communication). Mine tailings spread throughout the area may be associated with high concentrations of metals such as As, Cu, Hg, Pb, W, and Zn (Sullivan and Drever, 2001; Kim *et al.*, 2007; Twitty, 2007). Transport and dissolution of these metals by surface water can cause pollution downstream, especially worrisome where toxic heavy metals such as As, Hg, and Pb are present (Bell and Donnelly, 2006). Low pH associated with acid mine drainage through the oxidation of sulfide minerals, chiefly iron pyrite, leads to reduced solubility of these metals and their precipitation out of solution in streambed sediments (Kim *et al.*, 2007; Bradley, 2008). However, acidic drainage is uncommon in Colorado because of the presence of alkaline carbonate bodies buffering sulfide oxidation (Murphy *et al.*, 2000). Also, fire increases the content of alkaline oxides in

stream sediments and waters, further increasing this buffering effect and raising pH (Certini, 2005).

Mercury amalgamation was used in the reclamation of gold in the 1860s at Fourmile (Twitty, 2007). While this activity elevates Hg concentrations in Fourmile sediments, it appears to be a minor constituent, possibly due to the removal of Hg through volatization during wildfire (Biswas *et al.*, 2007; Beganskas, 2012). Furthermore, the use of Hg amalgamation in gold mining was short lived in Boulder County, with mechanical and smelting methods of concentrating pyretic and telluride gold ore becoming more prevalent after the initial boom of free-gold mining in the early 1860s (Twitty, 2007).
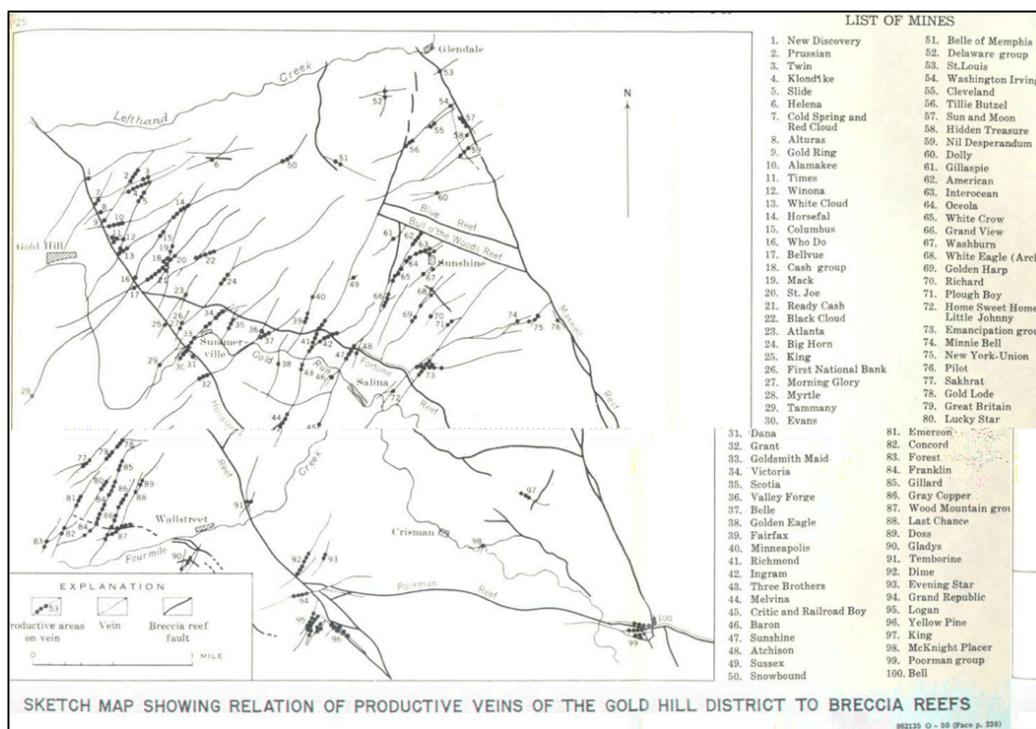
Figure 1.7. Late 1800s to early 1900s mining activity around Gold Hill in Fourmile Canyon. Productive intrusive ore veins trending northeast-southwest are associated with Laramide Breccia Reef faults trending northwest-southeast (Lovering and Goddard, 1950).

1.10. The 2010 Fourmile Fire

On September 6, 2010 a fire ignited near Emerson Gulch in Fourmile Canyon. The fire burned for 10 days covering a total area of 25 km^2 before being contained on September 13th (Fig. 1.8; Graham *et al.*, 2012). The fire was preceded by above normal temperatures and below normal rainfall in August (less than half the average precipitation) creating a short-term drought in early September (Ebel *et al.*, 2012; Graham *et al.*, 2012). The fire burned 14.5 km^2 within the Fourmile Creek Watershed in a mosaic pattern of low (2.6 km^2), moderate (9.4 km^2), and high (2.5 km^2) severity (Fig. 1.8). This exposed numerous tailings piles and waste rock associated with historical mining to rainfall and erosion (Fig. 1.9). The 2010 Fourmile Fire resulted in 169 homes destroyed and $217 million in damages (Writer and Murphy, 2012).
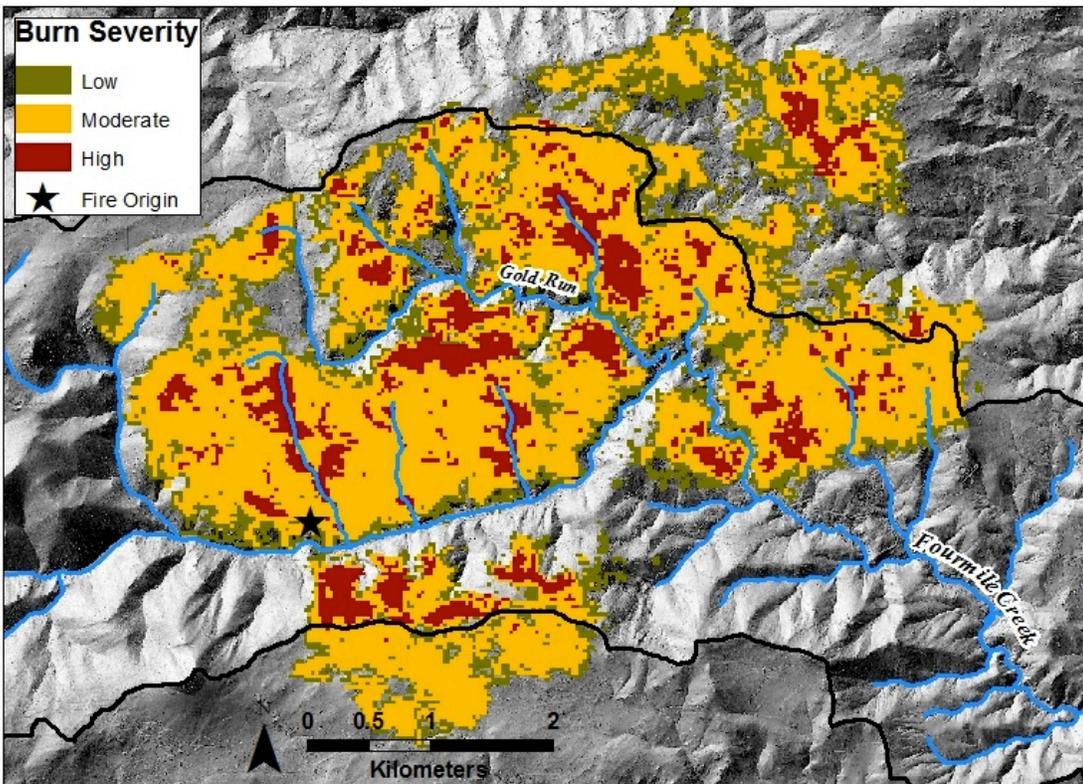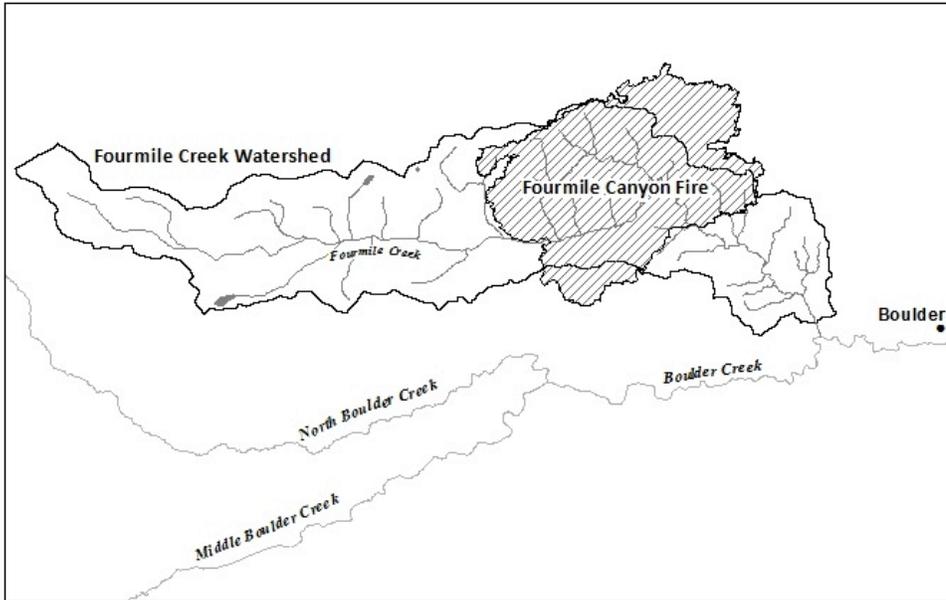
[Boulder: ESRI ArcGIS Online; Hydrography: USGS; Watershed: USGS StreamStats; Burn Severity
and Fire Perimeter: Boulder County GIS; Hillshade: Colorado University, Boulder CZO]

Figure 1.8. Fourmile Fire perimeter (top panel) and burn severity map (bottom panel). Fire spatial data courtesy of Boulder County GIS.

Figure 1.9. Tailings piles associated with mining activity exposed by wildfire. Photo taken July 2011 courtesy of S. Beganskas.

1.11. Previous Research

B. Ebel, J. Moody, and D. Martin of the U.S. Geological Survey examined the effect of the fire on soil properties and hydrology. The upper 3 cm of burned soil was 19% gravel, 67% sand, and 15% silt and clay, with 20–50% less organic carbon than unburned controls (Ebel *et al.*, 2012). Ash thickness was 0.1–8 cm due to wind redistribution prior to the first rainfall, with an average thickness of 1.8 cm and bulk density of 0.77 g/cm^3 (Ebel *et al.*, 2012; Moody and Ebel, 2012). This wettable ash was capable of storing 0.6 mm of water for each 1 mm of thickness, causing a lagged runoff response from the first October 2010 rain event (Moody and Ebel, 2012). Hyper-dry conditions present shortly after the wildfire and before the first rain events resulted in burned soils with 0.0087 cm^3/cm^3 volumetric water content, as opposed to unburned soils with 0.019 cm^3/cm^3 (Moody and Ebel, 2012).

J. Writer and S. Murphy of the U.S. Geological Survey carried out preliminary impacts on basin hydrology and stream chemistry in the year after the Fourmile Fire. Rainfall intensity and peak discharge were examined to determine the runoff effects in the first summer after the fire (Murphy *et al.*, 2012). A peak discharge of 23 m^3/s,

19

three times larger than the previous peak on record, was measured in Fourmile Creek on July 13, 2011 (Murphy *et al.*, 2012).

Writer *et al.* (2012) carried out frequent water sampling of Fourmile Creek the summer following the fire. Results indicated peaks in dissolved organic carbon and nutrients, such as nitrate, during summer storms, with potentially detrimental impacts on water quality. Additionally, elevated levels of Al, Fe, and Mn were noticeable in water samples, although none exceeded EPA regulated concentrations (Writer and Murphy, 2012). These nutrient fluxes were responsible for an increase in stream biofilm observed following the fire (Writer *et al.*, 2012). Additionally, fine sediment mobilized by the large rain events was remobilized by much smaller rain events, causing continued concerns for water quality (Writer *et al.*, 2012).

S. Beganskas (2012) undertook a study of the combined geochemical impacts of mining and wildfire on the water and sediment chemistry of Fourmile Creek shortly after a large July 2011 storm. This study quantified the disturbance in each sub-basin associated with mining and burn severity, along with bedrock distribution, as a basis for evaluating geochemical differences in water and sediment samples. Water samples indicate a positive correlation between both mining and fire with increased SO_4^{2-}, NO_3^-, and major cations. Both conductivity and Ca^{2+} concentrations increased through the burned area. Mining disturbance correlated positively with stream concentrations of Al, Cd, Co, Cr, Cu, Fe, Mn, and Zn. Stream sediment samples from burned drainages contained elevated major oxides and decreased SiO_2.

There has been limited research on postfire sediment yield in Fourmile Canyon. Ruddy *et al.* (2010) provided an emergency assessment of debris flow risks

to Fourmile Canyon. The report concluded a greater than 60% risk of severe erosive

events 1–3 years after the fire in a few severely burned drainages, with the potential

for about 20,000 m^3 of total sediment delivery. Despite limited study, sediment yield

produced by two years of fire-associated flooding is evident in channel deposits

downstream of the fire area (Fig. 1.10 & 1.11).

Figure 1.10. Fourmile Creek
upstream of fire. Note lack of
channel bank fine deposits. Photo
taken August 4, 2012.

Figure 1.11. Fourmile Creek downstream of
fire. Abundant overbank fine deposits and
woody debris buildups present from two
summers of flooding and sediment delivery.
Turbid water caused by rain on July 30
remobilizing fine sediment. Photo taken
August 3, 2012 courtesy of W. Ouimet.

1.12. Purpose of this Study

The present study focuses on movement of sediment and large-scale

hydrologic changes to Fourmile Canyon in the two summers since the fire. USGS

hydrology data from two stream gauges located in Fourmile Canyon are utilized in

conjunction with rain data from multiple sources to analyze Fourmile Creek's

discharge response to rain events of various intensities. Sediment storage and yield,

brought by postfire flooding, is calculated from field measurements and observations

of overbank channel deposits along Fourmile Creek and alluvial fans draining sub-basins.

In addition to this hydrologic and sediment yield analysis, several methods of tracing are employed to determine the movement of sediment in this drainage. Alluvial stratigraphy and overbank flood deposits, interpreted by geochemical and grain-size methods, can display the delivery of sediment from burned hillslopes and recovery since the fire. Geochemical analyses also display the influence of mining on sediment chemistry, important for assessing possible water quality impacts. As different peak discharges created two distinct sets of flood deposits (2011 and 2012) along the channel banks, differences in sediment chemistry and grain-size are assessed between these two years of sediment delivery. Long-term impacts of wildfire on Fourmile Canyon are considered using reasonable assumptions about fire and flood recurrence.

One complicating factor is that Fourmile Canyon is not a pristine study site. Over 150 years of settlement has left its mark on this watershed. Miners reworked many terrace surfaces along Fourmile Creek in their search for gold. This, combined with the presence of two flat grades on either side of the channel (the modern road and historical railroad) running the entire length of the burned area, creates a decoupled geomorphic drainage system. The hillslopes on either bank of Fourmile Creek are not directly connected to the main stem channel because of anthropogenic alteration.

2. Methods

2.1. Field Work and Sample Collection

Field observations, measurements, and sample collection took place in July and August 2012. Observations were recorded through notes and photos, providing insight into anthropogenic impacts and sediment transport in Fourmile Canyon. Samples included channel bank deposits from upstream and overbank deposits from downstream of the fire, ash samples, samples of coarse material from some of the gullies, and samples of bedload material from Fourmile Creek.

The largest flood of 2012 had a peak discharge of 3.7 m^3/s in Fourmile Creek (USGS Surface-Water, 2012). As this was well below the 2011 23.2 m^3/s record discharge (USGS Surface-Water, 2012), two distinct flood deposits were created along Fourmile Creek. The 2011 flood deposited sediment far from the channel, and, undisturbed by subsequent flooding, these deposits were covered by a thin organic litter layer. Sampling was accomplished by clearing the litter and removing the top ~5 cm of sediment. In other cases, the 2011 flood caused the buildup of woody debris around trees far from the channel and fine sediment caught in these debris dams was sampled (Fig. 2.1). The 2012 flood deposits were deposited near the channel and had not accumulated litter cover. Samples were taken from the top ~5 cm of this sediment (Fig. 2.2).

Figure 2.1. 2011 overbank deposits sampled in July 2012. Sampled sediment picked from woody debris pile up. Distance from channel indicates deposition during July 13, 2011 flood.

Figure 2.2. 2012 overbank deposits sampled in July 2012. Proximity to channel and lack of litter cover indicates recent deposition.

Measurement of the widths and depths of these overbank deposits, along with area and depth approximations of gully fans, were made in order to calculate 2-year fire-associated sediment storage. Trenching of overbank deposits was carried out in a few locations to observe flood deposit stratigraphy, which was also sampled. Valley floor maps were created for three areas of Fourmile Creek. These incorporated field measurements and observations of 2011 and 2012 flood deposits, recent gully fan deposits, Quaternary fan deposits, Quaternary terrace levels, and anthropogenic influence (chiefly mining). The geomorphic maps drafted in the field were later rendered in ArcGIS.

2.2. Hydrologic Analysis

Two USGS stream gauges operated seasonally from April–October exist along Fourmile Creek (Fig. 2.3). The first gauge, located within the burned area 5.8 km upstream of Boulder Creek, was installed in 2011 (Station 06727410, denoted

hereon as FCLM). The second stream gauge, located near the mouth of Fourmile

Creek (Station 06727500, denoted hereon as FCBC), has a historic record of daily

mean flow for 1947–1953, 1983–1995, and 2011–2012 (21 years in all).

Instantaneous discharge measured at 15-minute intervals is available at FCBC from

1987–1994. Instantaneous discharge measured at 5-minute intervals is available at

both FCBC and FCLM for 2011 and 2012.

Three sources of rainfall data exist for Fourmile Canyon (Fig. 2.3). The

National Atmospheric Deposition Program (NADP) operates a rain gauge near

Fourmile Canyon with records back to 1987, although this only records total 24-hour

precipitation. The University of Utah operates another rain gauge with data going

back to 2001 (MesoWest, 2012). This gauge records accumulated precipitation every

hour. The most precise rainfall data sources are seven tipping-bucket gauges operated

by the Urban Drainage and Flood Control District (UDFCD) since 1999. Located in

and around the Fourmile Fire perimeter, these gauges record incremental precipitation

at a very high frequency during storms.

The hydrograph and rainfall data provided by these gauges are used to

determine postfire changes in discharge characteristics, runoff response, mean daily

flow, flow duration, and flood recurrence in the pre- and postfire periods. The

creation of dimensionless hydrographs, by dividing discharge by peak discharge and

time by the total time base of the original hydrograph, is used to characterize the

differences in hydrographs from different sized storms.

Rainfall intensities calculated from the seven UDFCD gauges are used to

create rainfall intensity and amount maps in ArcGIS and determine runoff response in

Fourmile Creek from hydrograph data. The recurrence intervals of rain events are gathered from previous studies (D. Dethier, personal communication; Hershfield, 1961; Miller *et al.*, 1973). Limited overlap between high frequency rainfall sampling and high frequency discharge sampling restricts the rainfall-runoff analysis to the postfire period.
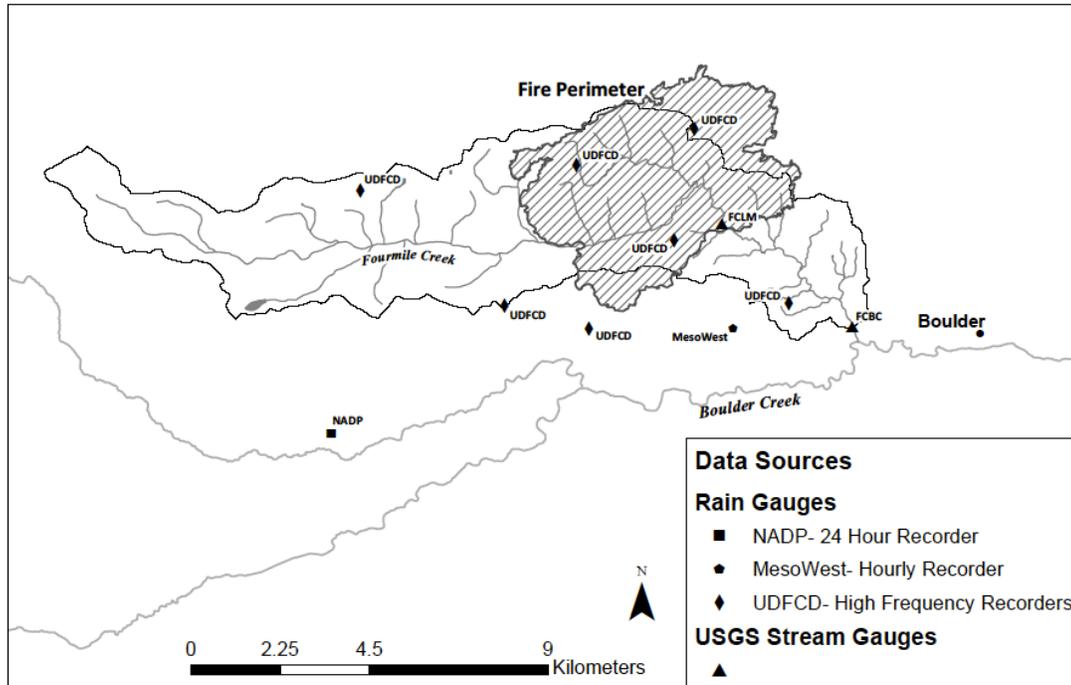
[Boulder: ESRI ArcGIS Online; Hydrography: USGS; Watershed: USGS StreamStats; Fire Perimeter: Boulder County GIS]

Figure 2.3. Gauge locations for discharge and rainfall used in this study.

2.3. Lab Work

Samples were initially dry sieved to measure fractions <2 mm, 2–4 mm, 4–9.5 mm, and >9.5 mm. The >2 mm fraction was stored, and all subsequent analyses took place on the <2 mm sample fraction. Near channel overbank deposits from within and downstream of the fire perimeter were amalgamated to create a 2011 and a 2012 floodplain sample.

All samples were oven dried overnight at 80° C and then placed into a furnace at 550° C for 3 hours. Loss on ignition (LOI), representative of sample organic matter content, was calculated as the percent loss in weight after furnace treatment. Following this, samples were taken to Southern Connecticut State University for grain-size analysis on the <2 mm fraction through a Horiba LA 950 laser diffraction particle size analyzer (J. Tait, personal communication). Samples were also observed under a standard binocular microscope to determine general mineralogy, clast angularity and charcoal abundance.

A number of samples were delivered for commercial analysis by inductively coupled plasma mass spectrometry and emission spectroscopy (ICP-MS & ICP-ES). This provided major, minor, and trace element data on the <150 μm fraction. Additional samples, with overlap from the commercially run samples, were analyzed for major oxides and trace elements by x-ray fluorescence (XRF) on a Bruker S4 Pioneer at Wesleyan University. The <2 mm fraction of these samples was initially ground into a fine powder using a shatterbox. All samples were then fired at 1040° C for 30 minutes in order to remove carbonate (J. Varekamp, personal communication). Overnight drying at 80° C took place again to ensure no water content prior to the creation of XRF discs.

XRF analysis of major oxides required the creation of glass discs by combining one part dried and powdered sample with five parts flux (47% lithium tetraborate, 37% lithium carbonate, and 16% lanthanum oxide). This amalgamation was placed in a platinum crucible and then a furnace heated to 1040° C. The molten sample was stirred after 3 and 5 minutes, poured and pressed into a glass disc after 8

27

minutes, then left overnight to cool to prevent cracking. A few samples were also run on the XRF for trace elements. Trace discs were created by combining each gram of sample with one binding agent bead for a total of 7–10 g of material. This material was placed in an aluminum cup and pressed under 15 t of pressure for 4.5 minutes to create the final discs. All sample runs contained duplicates and multiple standards to check accuracy.

Radionuclide analysis to determine ^{137}Cs and ^{210}Pb activity was carried out at two locations on the <2 mm sample fraction. An initial batch of three ash samples was sent to Rensselaer Polytechnic Institute for radionuclide gamma counting on a well counter (R. Bopp, personal communication). The remaining samples were sent to The College of William and Mary to complete radionuclide analysis on a gamma spectrometer (H. Mondrach, personal communication), with one sample from the first batch sent for recounting at William and Mary to check accuracy.

3. Results

3.1. Field Observations

Two years of flooding and sediment deposition in Fourmile Canyon has produced unique features, best enumerated by qualitative description. Overbank sediment deposits brought by flooding were found throughout the valley floor within and downstream of the fire area. These deposits ranged in thickness from a few centimeters to tens of centimeters (Fig 3.1). High water marks from recent flooding were observable in charcoal-rich debris deposited many meters from the channel (Fig 2.1) and by sediment high water marks left by turbid peak flows on bridge pylons along the channel reach. In contrast, upstream of the fire area fresh overbank deposits and signs of recent flooding were absent (Fig. 1.10).

Figure 3.1. Overbank fine deposits typically found within and downstream of burned perimeter associated with summer flooding. Photo taken August 2, 2012.

Common within the fire area were thick alluvial fans at gully mouths, some of which exceeded 50 cm in thickness near the gully mouth (Fig. 3.2). These deposits indicate downslope transport of sediment in runoff and subsequent deposition as thick, lobate fans on the valley floor. Debris flows created by the July 13, 2011 storm were likely responsible for much of this deposition (Beganskas, 2012). The fans were

29

localized below high-severity burned slopes and often extended to the channel to merge with overbank deposits. In places, the fans were found draped over the railroad grade on the south bank of Fourmile Creek and had not been transported to the valley floor by rain events. These fans also formed on the north bank, however, since Fourmile Drive runs along this edge of the stream, they were quickly excavated and removed before any measurements could be made.

Figure 3.2. Typical fan deposit seen at gully mouths throughout burned area. Thickness near mouth is ~30 cm here, tapering towards channel and merging with overbank deposits. Photo taken August 3, 2012 courtesy of W. Ouimet.

New rilling on the hillslopes was not apparent following any of the rain events in the two summers since the fire (J. Writer, personal communication). But, while new rills and gullies were not created, old ones were excavated by rainfall. This was evident in the incision of one gully (Banana Gulch) about 0.5 m into the railroad grade on the south bank of Fourmile Creek, along with numerous gullies stripped down to bare bedrock.

An alternating stratigraphy of thick, brown, sandy layers and thin, black, silty layers in trenched overbank deposits (Fig. 3.3) results from deposition in the waning stages of large discharge events. As peak flow declines with decreasing shear stress of the water, thick sand layers are deposited. As flow continues to recede the finer

suspended sediment is deposited as the thin silty layers. Given the prevalence of highly buoyant charcoal in these silty deposits very low flow, and perhaps ponding, must be required for their deposition (Meyer and Wells, 1997). The presence of pyrogenic material in nearly all overbank samples indicates the importance of burned hillslope regolith to this stratigraphy.

Figure 3.3. Overbank and gully deposit alternating stratigraphy observed within and downstream of burned area. Photos taken July and August 2012. Top left and top right courtesy of W. Ouimet.

A tour of the severely burned north-facing hillslopes monitored by the U.S. Geological Survey (Ebel *et al.*, 2012; Moody and Ebel, 2012) gave insight into the current state of erosion and recovery. The return of waist-high grasses and shrubs and stripping of ash deposits among groves of torched Douglas fir and Limber Pine on moderate to steep slopes was the most notable feature (Fig. 3.4). Despite this ground cover, eroding ash deposits are still apparent throughout the area (Fig. 3.5). A plot on a ~15° slope covered by a tarp to prevent erosion was uncovered in July 2012 by the USGS allowing for sampling of *in situ* ash (Fig. 3.6).

Figure 3.4. Return of grasses and shrubs among severely burned trees. Photo taken July 23, 2012 courtesy of W. Ouimet.

Figure 3.5. Stripping of ash to gravelly soil after two summers of rainfall. Sparse ash deposits still remain on slopes. Photo taken July 30, 2012.

Figure 3.6. Uncovered USGS plot, *in situ* ash sampled from top few centimeters of observed pit. Photo taken August 31, 2012 courtesy of W. Ouimet.

3.2. Mapping

Valley floor maps were created for three areas along Fourmile Creek using field measurements and observations (Fig. 3.7). The furthest upstream is directly below the severely burned north-facing slope monitored by the USGS (Site A. Wood Mine/Banana Gulch), the second site is downstream of Gold Run near the eastern burn perimeter (Site B. Logan Mill), and the final area is downstream of the fire perimeter (Site C. Arkansas Gulch). Mapping displays artificial grades on both banks constraining the channel along with mining-associated features including reworked terraces, levees, and tailings piles. Two Quaternary terraces were mapped with T1 being apparently older at about a 1.5 m height above the channel versus T2 at a height of about 0.5 m. An additional Quaternary feature were lobate fans of older material emanating from gully mouths. Fire-associated gully fan deposits are only apparent at Sites A and B within the burned perimeter, and do not occur downstream of Site B. Overbank deposits associated with the postfire flooding are not depicted on the map to reduce clutter, but were measured extensively in the field. These appeared as parallel bands on either side of Fourmile Creek running the entire length of the channel from downstream of the western fire perimeter (Fig. 3.1).
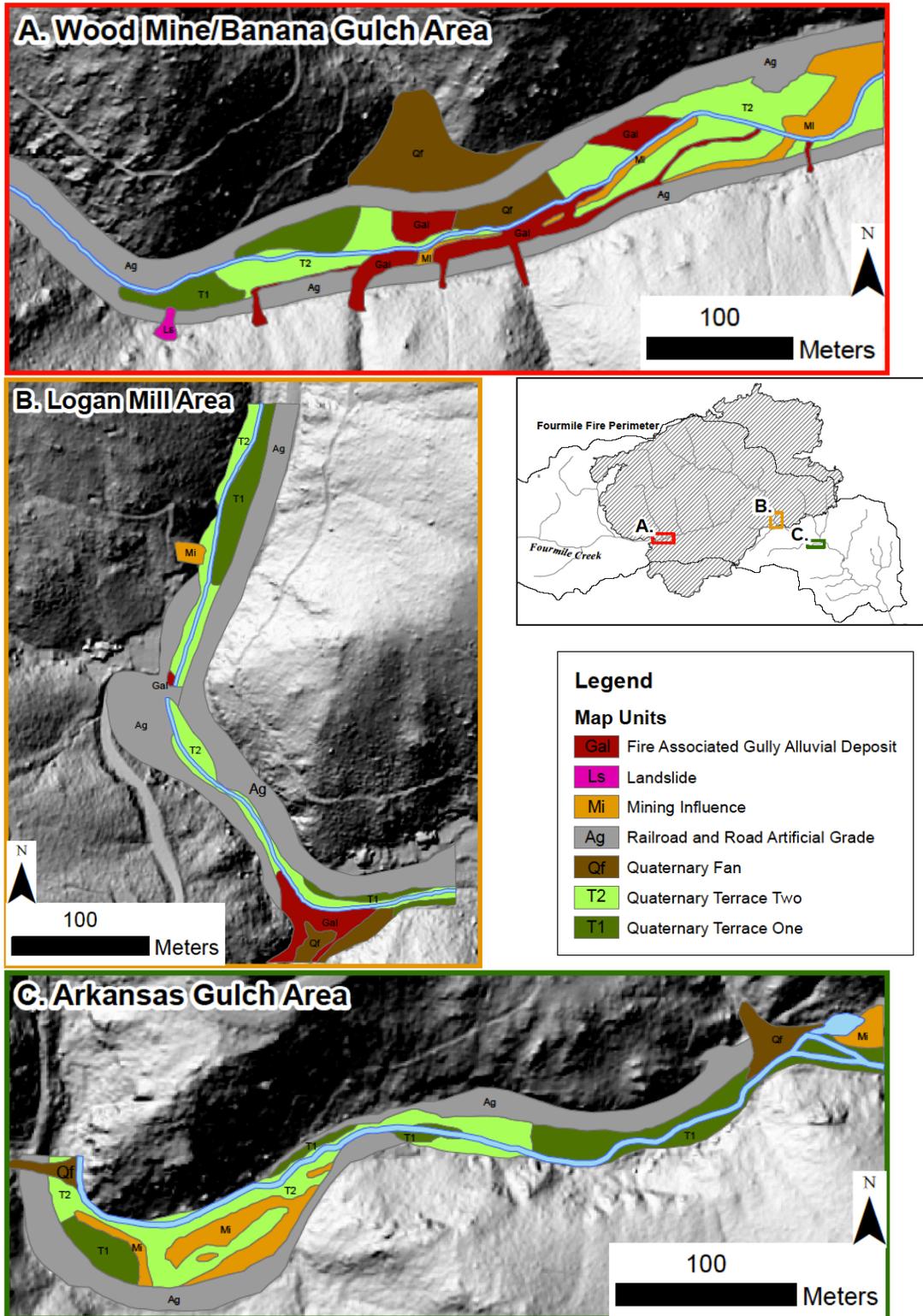
Figure 3.7. Valley floor maps rendered in ArcGIS for three areas along Fourmile Creek. Two within burned perimeter (A & B) and one downstream of burn (C).

3.3. Sediment Budget

Sediment budget refers to the balance of total sediment yield with sediment storage and sediment lost to throughput. This is used to quantify the erosion associated with the postfire flooding.

3.3.1. Sediment Storage

Area and depth measurements of overbank flood deposits and gully fan deposits in the mapped reaches allow for approximations of sediment storage within each reach (Table 3.1). Conversion from m^3 to t of sediment was accomplished using an average eroded sediment density of 1.7 t/m^3 (Moody and Martin, 2009).

Table 3.1. Approximate sediment storage with and without gully deposits for each channel reach mapped in Figure 3.7.

Site	Length of Reach (m)	Channel Bank Storage (t)	Total Storage Including Gully Deposits (t)
A. Wood Mine/Banana Gulch	1,400	1,020	3,910
B. Logan Mill	1,050	1,410	2,830
C. Arkansas Gulch	1,000	1,910	1,910

Channel bank storage increases downstream of the western fire perimeter as flood deposits widen (A<B<C), perhaps caused by higher flows experienced further downstream during flooding. The addition of gully deposits within the burned perimeter causes total sediment storage to decrease downstream (A>B>C) indicating the importance of these deposits to total storage. Extrapolating channel bank storage results of Site B upstream to the western fire perimeter and the results of Site C to the unburned downstream portion of Fourmile Creek yields an approximate total storage of 19,000 t of sediment from this fire event.

35

The estimated 19,000 t of storage within and downstream of the fire area is a low estimate. Channel bank storage was absent from reaches constrained by the railroad and road grades. Therefore, conservative estimates of flood deposit widths and depths were utilized in the extrapolation of mapped areas. Recent gully fan deposits found within the fire area beneath severely burned slopes were omitted as not all were mapped and measured. The potential storage of these fans is evident in their contribution to total storage at mapped sites: 75% at Site A and 50% at Site B (Table 3.1). Further subtracting from sediment storage were the many tonnes of sediment excavated and removed from Fourmile Drive.

Sediment stored along Gold Run's 5.4 km reach is also not included, as time in the field did not allow for detailed exploration of this area. The narrow valley of this drainage, dominated by Gold Run Road, also experienced significant removal and bulldozing of sediment delivered during rain events. Gold Run is a significant omission as 20% of its 7.1 km^2 drainage was burned at high severity, with 70% of its total area affected (Fig. 1.8; Beganskas, 2012).

3.3.2. Throughput

Throughput in the form of suspended fines rapidly flushed from the Fourmile Canyon Watershed also accounts for missing material from the sediment budget. This factor was evident in streamflow turbidity created for several days after rain events, as fine overbank deposits were remobilized and flushed further downstream (Fig. 3.8).

Figure 3.8. Turbid waters in Fourmile Creek caused by remobilization of overbank fine deposits. Photo taken August 3, 2012 four days after large July 30 rain event. Courtesy of W. Ouimet.

Total suspended sediment (TSS) measured at various locations in Fourmile Creek in 2011 by the USGS was used to create a TSS rating-curve for the postfire period downstream and upstream of the disturbed area (Fig. 3.9; J. Writer, personal communication). Limited data exist upstream of the fire, and, as expected, no high flows were measured here, so TSS remained low peaking at only 210 mg/L. On the other hand, TSS ranged up to 68,000 mg/L within the disturbed area where more sediment was available for transport and higher flows were experienced. High variability at low flows and limited data at high flows made determination of throughput for individual storms problematic. Using average discharge and a visual estimate of TSS from Figure 3.9A, the July 13, 2011 flood contributed approximately 1,700 t of sediment to throughput. It is therefore conceivable that several thousand tons of sediment have been flushed from the watershed in the two years since the fire.
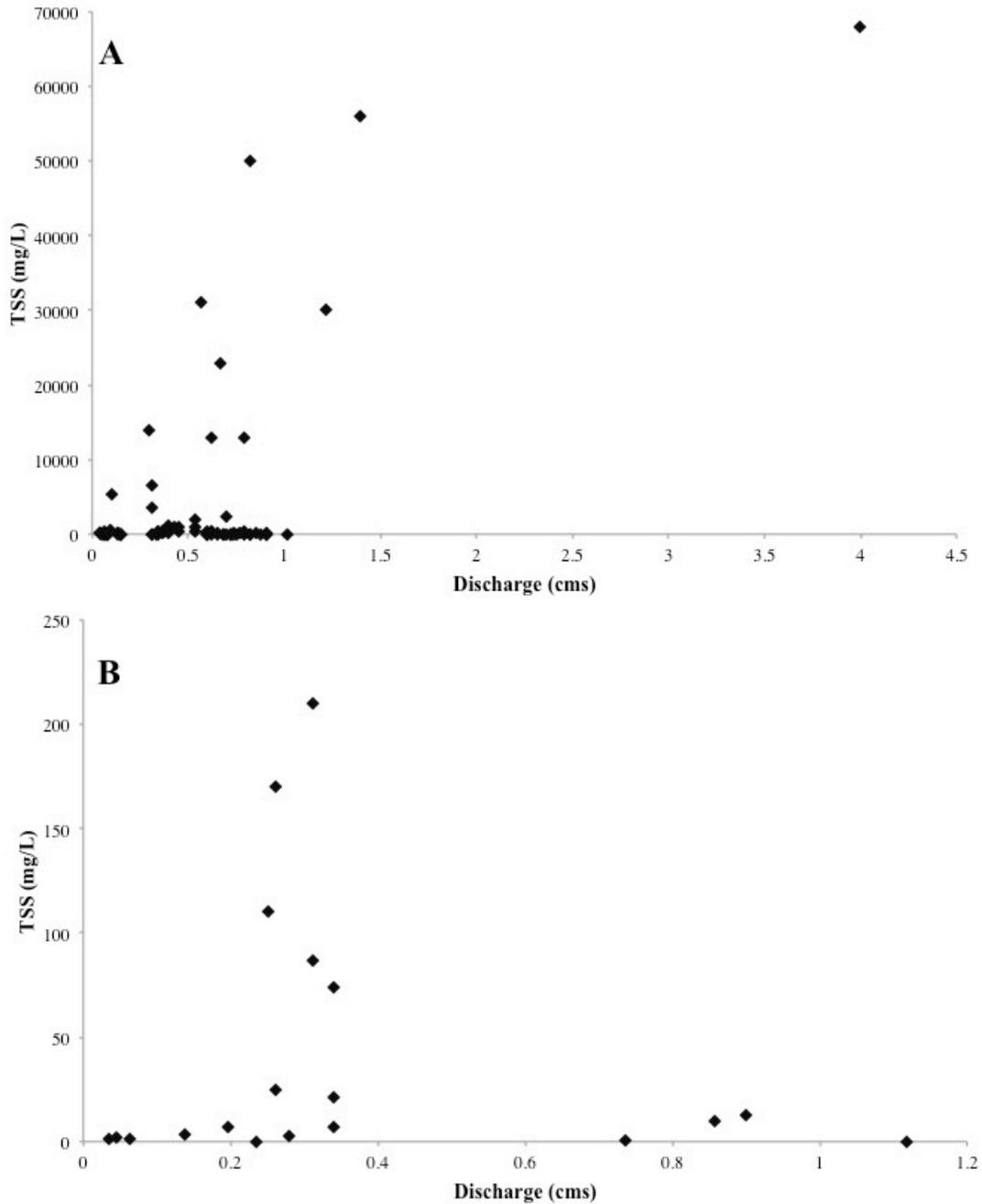
Figure 3.9. Total suspended sediment rating-curves downstream (A) and upstream (B) of the western fire perimeter. All data is from Spring and Summer 2011. Note the two order of magnitude increase in TSS scale for the downstream curve as more sediment is available and higher flows are experienced. Data courtesy of J. Writer (USGS).

3.3.3. Sediment Yield

Calculation of potential sediment yield from the entire burned area required extrapolation of available data. B. Ebel (personal communication) reports a July–August 2012 sediment delivery of 0.32 kg/m^2 for one high-severity burned hillslope plot. Assuming that the 2011 sediment delivery was three times this, because of increased availability of erodible sediment, then the two-year delivery from high-severity burned slopes is 1.28 kg/m^2. Assuming that moderate and low-severity burned slopes produced only 10% (0.128 kg/m^2) and 1% (0.0128 kg/m^2) respectively of the yield from high-severity burned slopes, it is possible to extrapolate two-year sediment delivery to the entire burned area. Given 2.5 km^2, 9.4 km^2, and 2.6 km^2 of area burned at high, moderate, and low severity respectively, the total potential sediment yield comes to 4,400 t. The assumptions used here are consistent with literature on rapidly decreasing hillslope yields observed with decreasing burn severity and increasing time since fire (Benavides-Solorio and MacDonald, 2005; Smith *et al.*, 2011b).

This yield does not account for the ash present on severely burned slopes immediately after the fire. These deposits have been largely eroded and transported downslope, as evidenced by field inspection of hillslopes in July 2012 (Fig. 3.5). Reported average ash thickness and density soon after the fire was 1.8 cm and 0.77 g/cm^3 respectively (Ebel *et al.*, 2012; Moody and Ebel, 2012). If this is assumed to represent all ash deposits on high-severity burned slopes, which cover an area of 2.5 km^2, then the potential contribution of ash to total sediment delivery is calculated at 35,000 t. This is an upper estimate, as evidenced by the presence of some un-eroded

ash deposits on hillslopes in 2012 and the potential overlap of ash-only input with extrapolated sediment delivery from high-severity burned plots.

The addition of ash to total sediment yield, as extrapolated from the 2012 data point, leads to a total potential yield of 39,400 t. Storage of sediment on slopes is ignored in these calculations, as the average 20° slope of this drainage suggests that slope storage is a minimal factor throughout Fourmile Canyon.

Ruddy *et al.* (2010) estimate approximately 20,000 m^3 of potential delivery under a 60% chance of debris flow in several severely burned gullies in Fourmile Canyon. This estimate relies on an empirical model accounting for slope, burn severity, and total storm rainfall. Using the 1.7 t/m^3 density estimate for eroded sediment, the mass of this potential debris flow sediment is 34,000 t. This value is comparable to the 39,400 t estimate used in this study.

3.4. Hydrologic Analysis

3.4.1. Streamflow Analysis

Elevated sediment delivery from severely burned slopes is tied to increased runoff from moderate rainfall events. These events are also responsible for elevated discharge in Fourmile Creek. The limited data on prefire streamflow and rainfall allows for some comparison to the postfire hydrology. The largest flood of 2011 occurred on July 13 with a peak of 23.2 m^3/s at the FCLM gauging station and 21.8 m^3/s at the FCBC station (see Fig. 2.3 for station locations), two floods on July 13–14 and July 14 immediately followed this as rainfall continued. These peaked at 5.6 and 2.7 m^3/s respectively at FCBC. The July 13 flood was three times larger than the next largest on record, a 7.3 m^3/s event on June 1, 1991, which was likely a rain-on-snow

event given the early June date and high baseflow (1.25 m^3/s; USGS Surface-Water, 2012).

On the other hand, the largest flood of 2012 occurred on July 30 with a reduced peak of 2.9 and 3.7 m^3/s at FCLM and FCBC respectively. A Log Pearson III analysis of the peak flow record for FCBC (1947–1953, 1983–1994, 2011–2012; 21 years) plots the 2011 flood as the 70-year event, the 1991 flood as the 10-year event, and the 2012 flood as the 5-year event (Fig. 3.10). A video feed operated by the USGS at the FCBC gauging station provides still images of the peak 2011 and 2012 floods (Fig. 3.11).
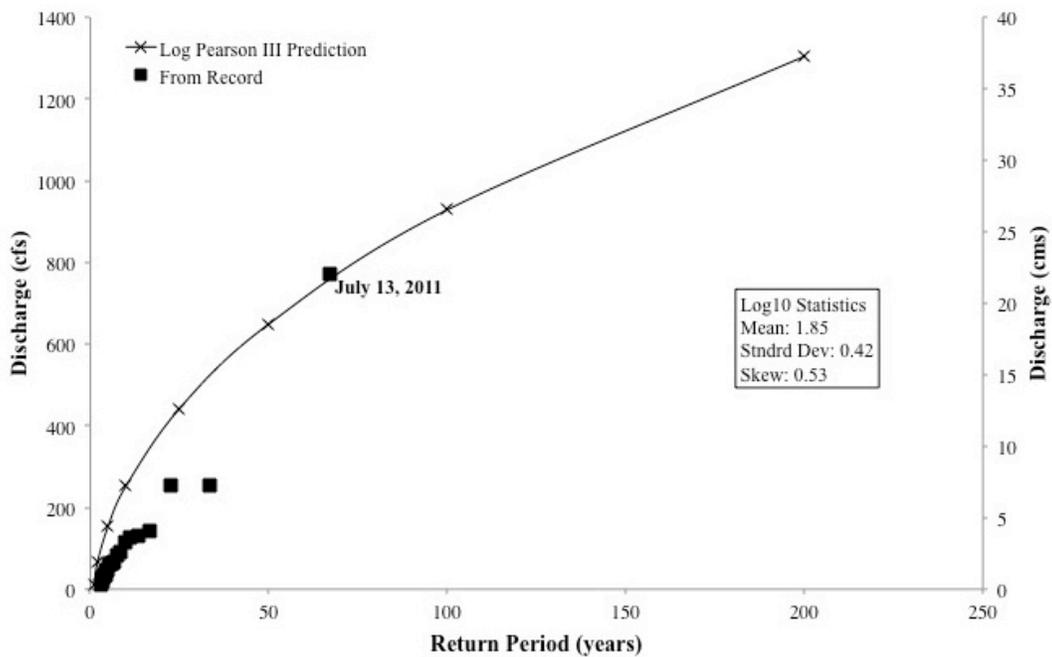
Figure 3.10. Log Pearson III flood return period analysis based on 21-year peak flow record at FCBC gauging station (USGS Surface-Water, 2012).

Figure 3.11. Flood stage at FCBC for 2011 and 2012 floods as recorded by USGS video feed. Note the 2011 flood was large enough to overtop the banks and flow into the adjacent parking lot.

These peak flows, along with other high flow events during both summers, increased July daily mean discharge of Fourmile Creek when compared with the prefire record (Fig. 3.12). Mean daily discharge for the full period of record is also plotted on a flow duration curve representing all 21 years of available data for the April 1st–September 30th pre- and postfire periods (Fig. 3.13). This data indicates that mean daily flows are considerably lower in the postfire period, with percent exceedences typically half their prefire values (Table 3.2).
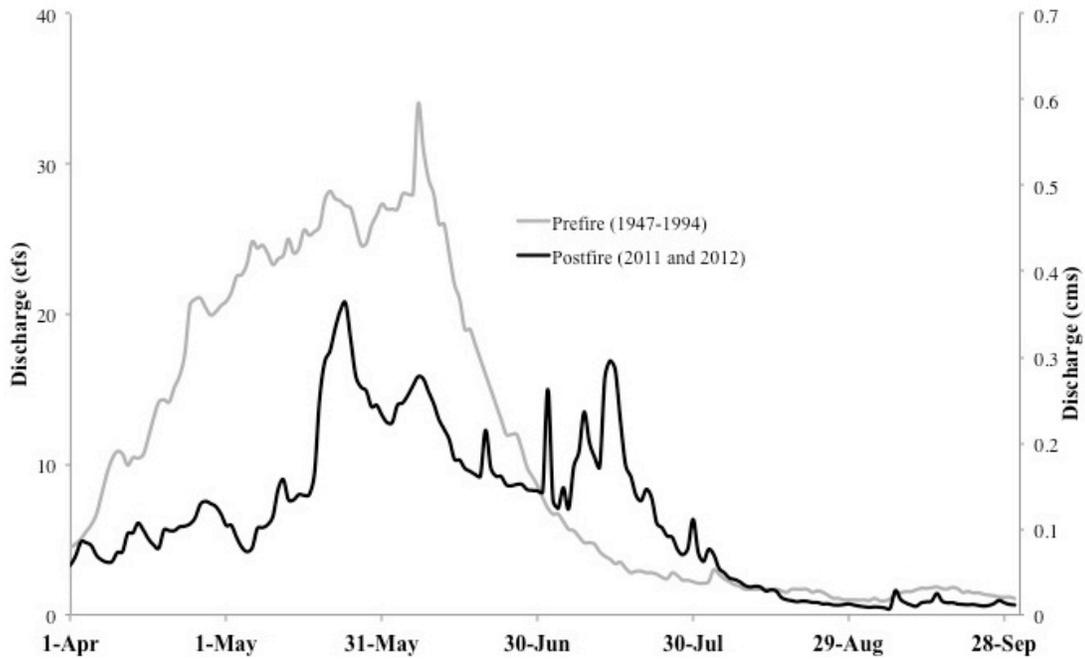
Figure 3.12. Mean daily discharge comparison for April 1st–September 30th records. High flows of July 2011 and 2012 produce higher mean July discharge in postfire period. Values converge with prefire discharge into August (USGS Surface-Water, 2012).
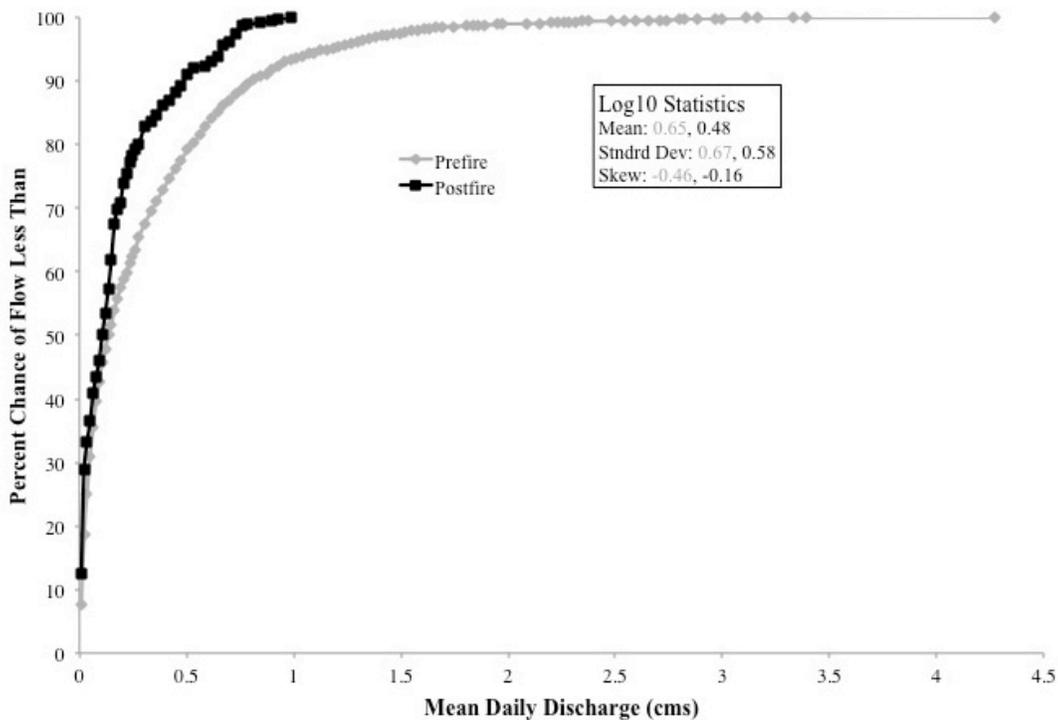
Figure 3.13. Flow duration curve for mean daily discharge pre- and postfire for April 1st–September 30th period (USGS Surface-Water, 2012).

Percent Exceedence (%)	Prefire (m^3/s)	Postfire (m^3/s)
1	2.095	0.814
5	1.161	0.658
10	0.807	0.488
20	0.524	0.276
25	0.425	0.219
30	0.340	0.177
40	0.219	0.142
50	0.135	0.106
60	0.078	0.064
70	0.050	0.021
75	0.035	0.020
80	0.023	0.014
90	0.011	0.006
95	0.007	0.003
99	0.003	0.001

Table 3.2. Percent exceedence flow values for pre- and postfire period based on flow duration curve in Figure 3.13.

Snowmelt discharge was not studied extensively because of complicating factors of timing and amount of winter snow. Despite half the average snowfall in the 2010–2011 winter, peak discharge in Spring 2011 was 1.08 m^3/s, exceeding the mean prefire peak snowmelt discharge of 0.96 m^3/s. On the other hand, the above average snowfall in the 2011–2012 winter resulted in a peak snowmelt discharge of only 0.34 m^3/s in Spring 2012 (High Plains Regional Climate Center, 2012; USGS Surface-Water, 2012). While 2011–2012 snowfall was high, the majority fell in December and February. Warm periods throughout the winter would have melted or sublimated much of this prior to spring runoff. On the other hand, large mid-May mixed rain- and snowstorms in 2011 resulted in a higher spring discharge despite less overall snowpack (S. Murphy, personal communication).

Selected hydrographs are utilized in assessing postfire summer hydrologic changes in Fourmile Canyon. Suitable prefire hydrographs are gathered from the

1987–1994 FCBC instantaneous record, whereas, both FCLM and FCBC hydrographs are gathered for the postfire period. Prefire hydrographs tend to have longer time bases, lower peak flows, and a longer time to rise of peak flows (Fig. 3.14) compared with postfire hydrographs (Fig. 3.15). The dual peaks seen in many prefire hydrographs are a unique feature of this basin (Fig. 3.16). Only three dual peak examples exist postfire, and the lag between peaks is much less (Fig. 3.17). Peak flow, time base, time to rise, and lag between peaks for pre- and postfire hydrographs are compiled in Tables 3.3 and 3.4 respectively. On average the time base of hydrographs in the postfire period is about two hours less than in the prefire, the time to rise occurs at about 9% of the total time base versus 15% prefire, and the lag between dual peaks is 45 minutes less during postfire runoff. Dimensionless hydrographs, used to assess time to rise of the original hydrographs, are averaged for the pre- and postfire period (Fig. 3.18), displaying the longer time to rise and dual peaked nature of the prefire hydrographs.
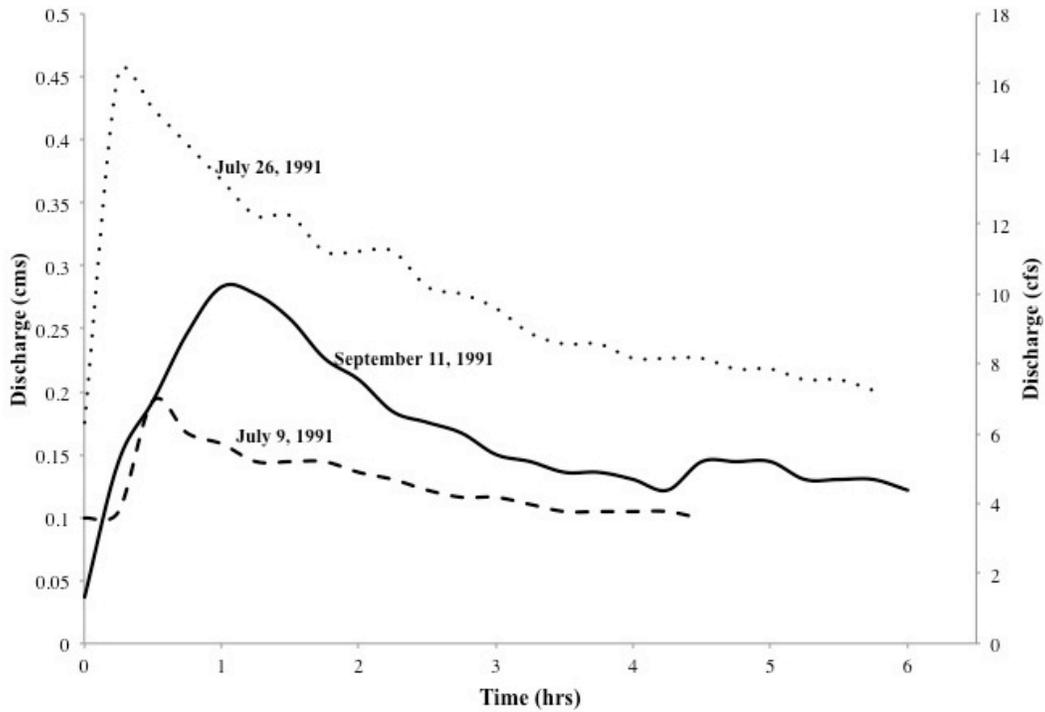
Figure 3.14. Example hydrographs from the prefire discharge record. Note the 6-hour time scale on the x-axis and 0.5 m^3/s discharge scale on the y-axis (USGS Surface-Water, 2012).
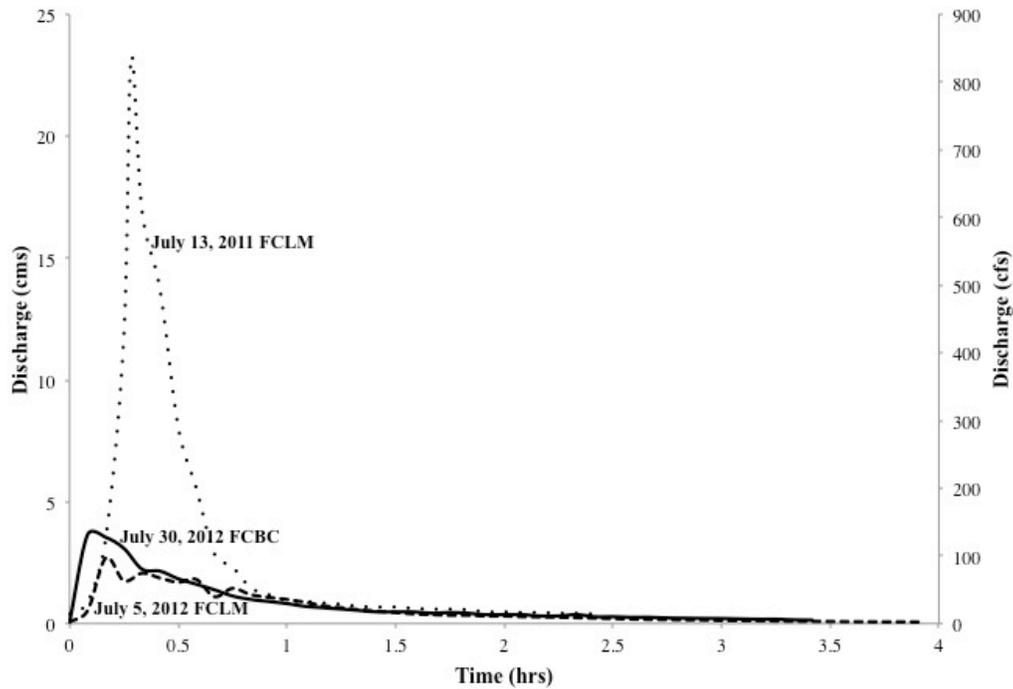
Figure 3.15. Example hydrographs from the postfire discharge record, with FCLM data included. Note the 4-hour time scale on the x-axis and 25 m^3/s discharge scale on the y-axis (USGS Surface-Water, 2012).
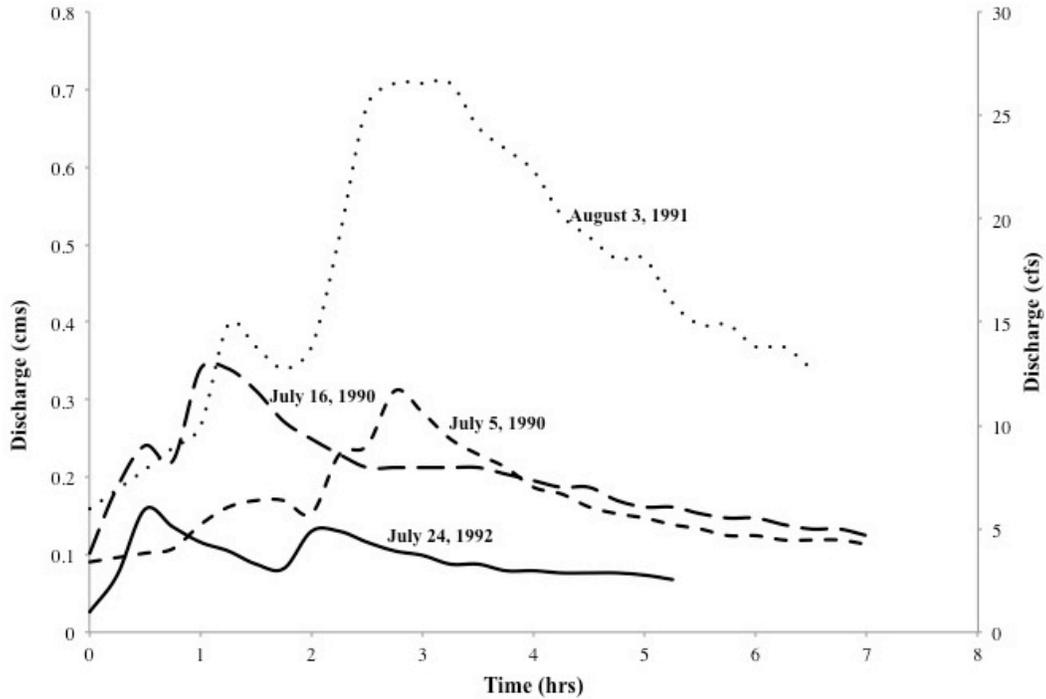
Figure 3.16. Example dual peak hydrographs from the prefire discharge record. Again note the 8-hour time scale on the x-axis and 0.8 m^3/s discharge scale on the y-axis (USGS Surface-Water, 2012).
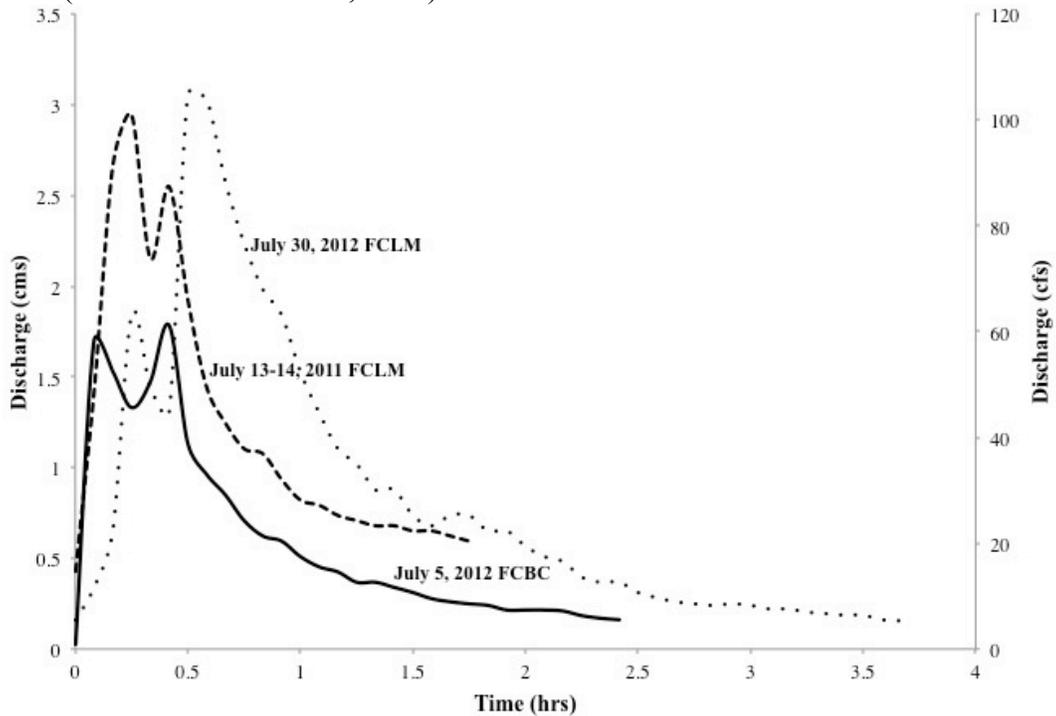
Figure 3.17. All dual peak hydrographs from the postfire discharge record, with FCLM data included. Again note the 4-hour time scale on the x-axis and 3.5 m^3/s discharge scale on the y-axis (USGS Surface-Water, 2012).

Table 3.3. Compiled prefire hydrograph data. Averages presented on bottom.

Date	Time Base (hrs)	Peak Discharge (m³/s)	Time to Rise (% of total time base)	Dual Peak (Y/N)	Lag Between Peaks (mins)
7/5/90	7	0.3	15	Y	60
7/16/90	7	0.3	14	Y	30
8/12/90	3	0.2	22	Y	45
8/16/90	4.5	0.3	11	Y	75
6/1/91	3.75	7.3	33	N	
7/9/91	4.5	0.2	11	N	
7/19/91	2.75	0.2	12	Y	30
7/22/91	5.25	0.7	14	N	
7/26/91	5.75	0.5	4	N	
8/3/91	6.5	0.7	21	Y	90
9/11/91	6	0.3	17	N	
7/24/92	5.25	0.2	10	Y	90
Average	**5.1**	**0.9**	**15**		**60**

Table 3.4. Compiled postfire hydrograph data. Data separated by hydrographs from FCBC and FCLM stations. Averages taken across both records. Lack of significant peak led to exclusion of June 20, 2011 event (Fig. 3.20, bottom). Insignificant discharge at FCLM led to exclusion of July 7, 2011 event there.

Date	Time Base (hrs)	Peak Discharge (m³/s)	Time to Rise (% of total time base)	Dual Peak (Y/N)	Lag Between Peaks (mins)
FCBC					
7/7/11	1.17	0.7	7	N	
7/13/11	2	21.8	9	N	
7/13-14/11	1.33	5.6	6	N	
7/14/11	2.58	2.7	6	N	
9/7/11	4	0.3	4	N	
9/14/11	6	0.1	11	N	
7/5/12	2.42	1.8	3	Y	20
7/30/12	3.42	3.7	2	N	
FCLM					
7/13/11	2.42	23.2	12	N	
7/13-14/11	1.75	2.9	14	Y	10
7/14/11	1.83	1.6	14	N	
9/7/11	3.42	0.4	20	N	
9/14/11	8	0.1	12	N	
7/5/12	3.92	2.7	4	N	
7/30/12	3.67	2.9	7	Y	15
Average	**3.2**	**4.7**	**9**		**15**
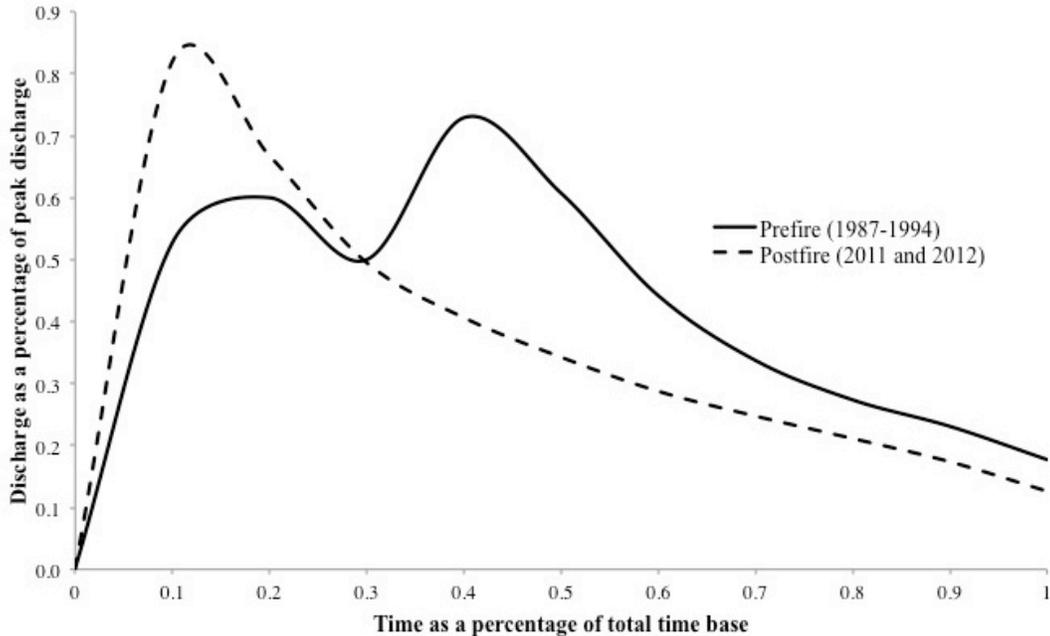
Figure 3.18. Averaged dimensionless hydrographs. Note the shorter time to rise, more peaked nature, and missing dual peaks of the postfire curve.

3.4.2. Rainfall-Runoff Analysis

Rainfall data from the UDFCD and NADP gauges (see Fig. 2.3 for station locations) associated with the aforementioned hydrographs is useful in assessing hydrologic conditions in the pre- and postfire period. Unfortunately, accurate rainfall data is only available for the postfire period from the UDFCD tipping-bucket gauges located in and around the fire perimeter. These are used to calculate maximum 30-minute rainfall intensities for each gauge to get an average basin-wide I_{30} in addition to total rainfall and amount-duration return periods. Prefire rain data is limited to the 24-hour NADP precipitation accumulation recorder, located several kilometers outside of the watershed. Therefore the spatial extent and duration of each storm is unknown, so I_{30} and return period calculations were not made. Available pre- and postfire compiled rainfall data can be found along with unit-area peak discharge in Tables 3.5 and 3.6 respectively.

49

Table 3.5. Prefire unit-area peak discharge and rainfall data gathered from NADP.

Date	Unit-Area Peak Discharge (m^3/s/km^2)	Total Rainfall (mm)	Effective Rainfall for Total Drainage (mm)	Averaged I_{30} (mm/hr)	Maximum I_{30} (mm/hr)	Amount-Duration Return Period (yrs)
7/5/90	0.0049	No data	0.03			
7/16/90	0.0054	5	0.04			
8/12/90	0.0032	No data	0.007	Prefire rain data from NADP rain gauge located well outside watershed. Spatial extent, duration, and rainfall intensity is therefore unknown.		
8/16/90	0.0054	14	0.03			
6/1/91	0.1151	44	0.55			
7/9/91	0.0030	No data	0.007			
7/19/91	0.0032	6	0.008			
7/22/91	0.0108	19	0.1			
7/26/91	0.0071	13	0.035			
8/3/91	0.0113	30	0.1			
9/11/91	0.0044	17	0.05			
7/24/92	0.0025	14	0.02			
Average	**0.0147**	**18**	**0.08**			

Table 3.6. Postfire unit-area peak discharge and rainfall data gathered from UDFCD. Data separated by gauging station (FCBC and FCLM) for unit-area peak discharge and effective rainfall, both dependent on upstream area. Long duration (~8 hrs) and low intensity led to exclusion of June 20, 2011 event (Fig. 3.20) and insignificant discharge led to exclusion of July 7, 2011 event at FCLM.

Date	Unit-Area Peak Discharge (m^3/s/km^2)	Total Rainfall (mm)	Effective Rainfall for Total Upstream Drainage (mm)	Effective Rainfall for Burned Area (mm)	Averaged I_{30} (mm/hr)	Maximum I_{30} (mm/hr)	Amount-Duration Return Period (yrs)
FCBC							
7/7/11	0.0113	17	0.01	0.03	22	48	1–5
7/13/11	0.3460	14	0.4	1.4	19	40	1–2
7/13-14/11	0.0881	4	0.1	0.3	31	43	1
7/14/11	0.0422	8	0.1	0.6	21	36	1
9/7/11	0.0044	16	0.03	0.06	7	8	1
9/14/11	0.0022	19	0.02	0.05	9	14	1
7/5/12	0.0283	15	0.08	0.2	27	55	1–5
7/30/12	0.0579	14	0.1	0.4	48	79	1–5
FCLM							
7/13/11	0.4644	Same as above	0.3	0.7	Same as above	Same as above	Same as above
7/13-14/11	0.0588		0.1	0.25			
7/14/11	0.0328		0.06	0.2			
9/7/11	0.0080		0.02	0.04			
9/14/11	0.0024		0.02	0.05			
7/5/12	0.0538		0.15	0.3			
7/30/12	0.0580		0.2	0.5			
Average	**0.0839**	**13**	**0.11**	**0.34**			

Effective rainfall, the rainfall that actually produced runoff, is extremely low, representing a minuscule fraction of total rain received. As the spatial extent of each storm for the prefire period is unknown, only total drainage area is used to calculate effective rainfall (Table 3.5). For the postfire period both total drainage area (63 km^2 at FCBC or 50 km^2 at FCLM) and approximate spatial extent of each storm over the burned area are used in these calculations (Table 3.6). While using the smaller storm area triples the average effective rainfall, the order of magnitude of both results is equally small (10^{-1} mm). The spatial extent of the storm over the burned area is likely more accurate given previous studies finding little runoff produced on undisturbed slopes from rain events that produced significant runoff and floods in burned drainages (e.g. Elliot and Parker, 2001).

Although limited comparison is possible between pre- and postfire rainfall-runoff effects, the postfire data are useful in assessing the runoff response given storms of varying magnitude over the two summers since the fire. For instance, the July 13, 2011 flood had a unit-area peak discharge at FCBC of 0.346 m^3/s/km^2 given a total rainfall of 14 mm and average I_{30} of 19 mm/hr. On the other hand, while the total rainfall associated with the July 30, 2012 flood was identical at 14 mm and the average I_{30} was much greater at 48 mm/hr, the unit-area peak discharge at FCBC for this event was only 0.0579 m^3/s/km^2. A threshold I_{30} around 10 mm/hr is often determined as the critical value in significant runoff generation following wildfire (e.g. Moody and Martin, 2001a). Unit-area peak discharge plotted against average I_{30} displays that I_{30} values below 10 mm/hr don't appear to generate significant runoff in Fourmile Canyon, though there is a lack of data in the 10–20 mm/hr range (Fig. 3.19).
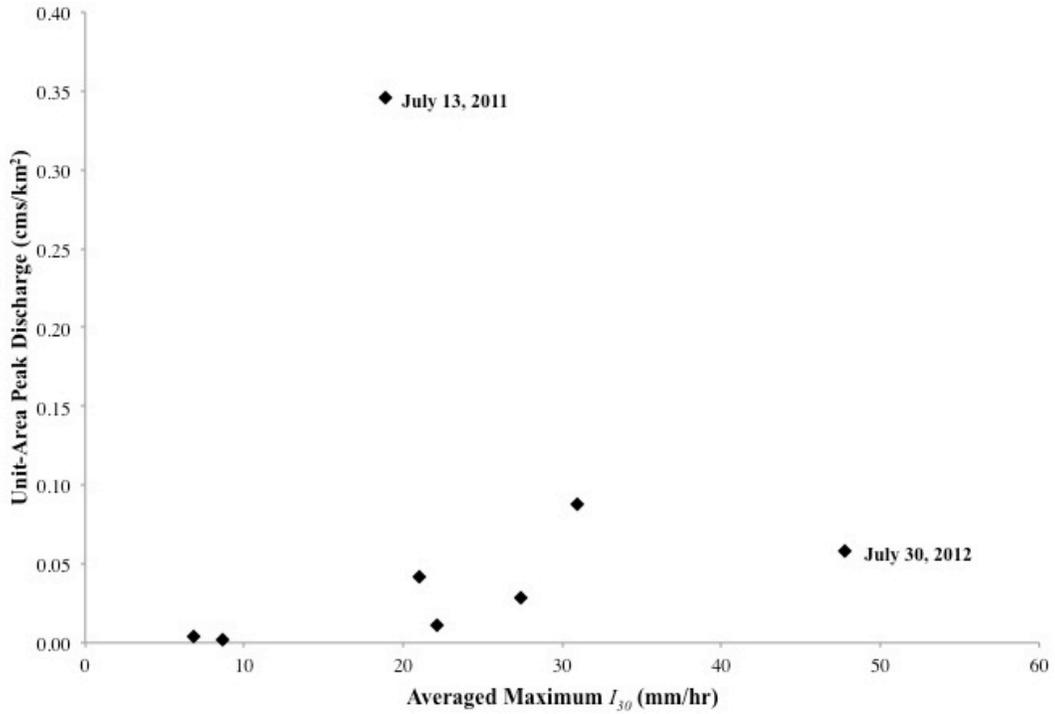
Figure 3.19. Unit-area peak discharge at FCBC plotted against basin-wide average I_{30} for 2011 and 2012 storm events. Despite missing data in the 10–20 mm/hr range, there appears to be an I_{30} cutoff within this, below which limited runoff is produced.

Rainfall maps produced using ArcGIS are examined in conjunction with hydrographs to assess the watershed's response to summer rainfall events since the fire. Despite high rainfall amounts on June 20, 2011, the low intensity of this event was ineffective in generating streamflow (Fig. 3.20). The July 7, 2011 storm was greater in intensity, but focused south of the watershed, thus generating very little discharge again (Fig. 3.21). The absorbent ash layer, capable of holding up to 11 mm of rainfall (Moody and Ebel, 2012), also contributed to insignificant discharge during these initial rain events. By the July 13, 2011 event the ash was likely saturated, underlain by hydrophobic mineral soil (Moody and Ebel, 2012). Thus, intense rainfall over severely burned portions of Fourmile Canyon created the conditions for the 70-year flood (Fig. 3.22). In 2012 intense rainfall events occurred twice over severely burned portions of Fourmile Canyon, yet only generated moderate runoff responses (Fig. 3.23 & 3.24).

June 20, 2011
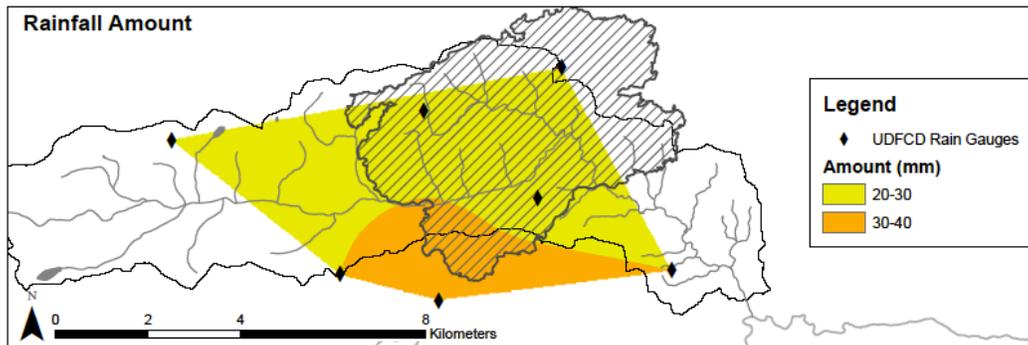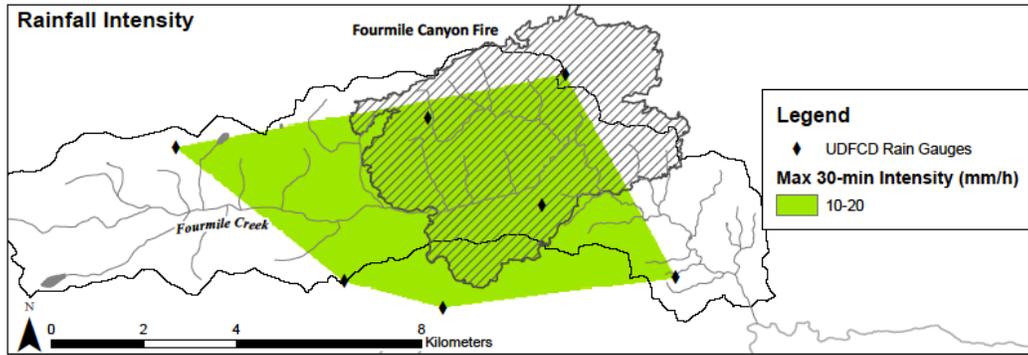
[Hydrography: USGS; Watershed: USGS StreamStats; Fire Perimeter: Boulder County GIS; Rainfall Gauges and Data: Urban Drainage and Flood Control District]
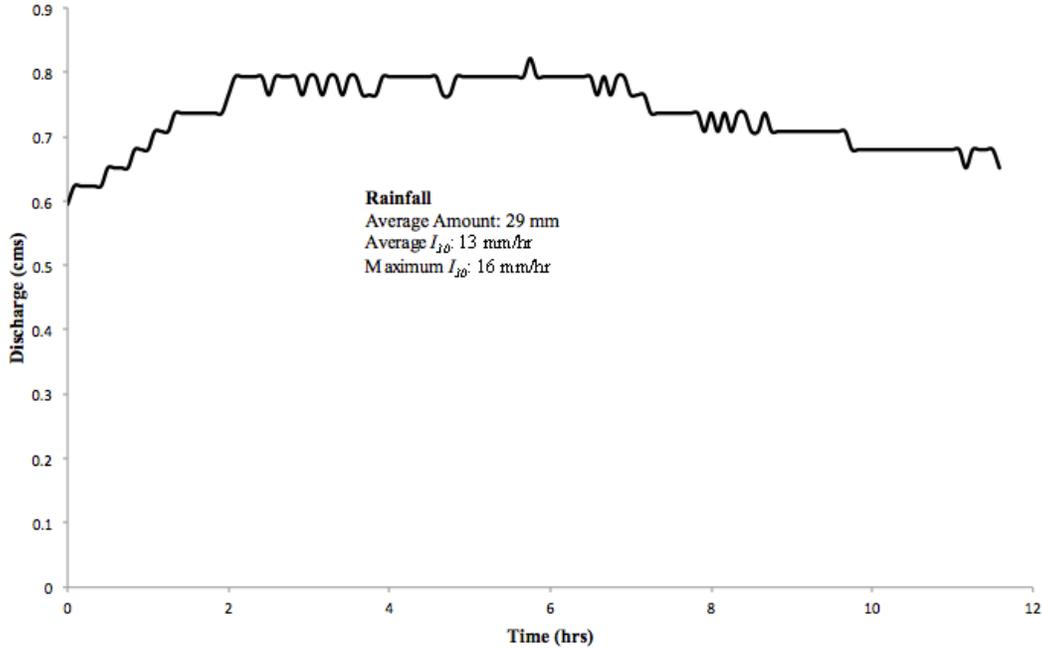
Figure 3.20. High rainfall at low, uniform intensity on June 20, 2011 generates low peak discharge of 0.82 m^3/s for the first major summer storm event following the September 2010 fire.

July 7, 2011
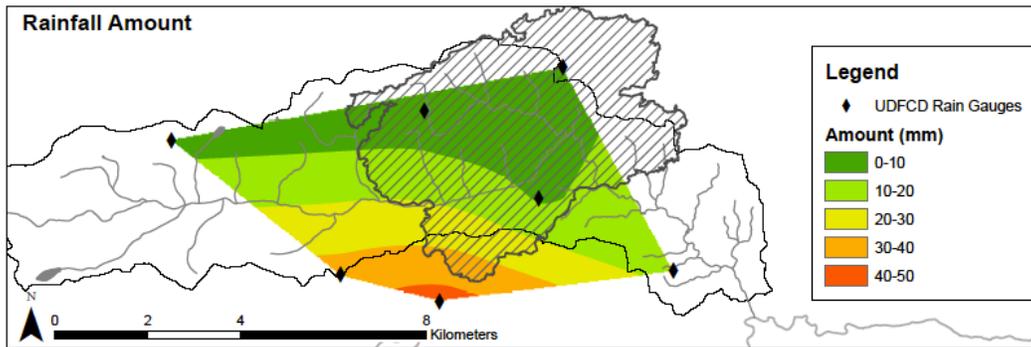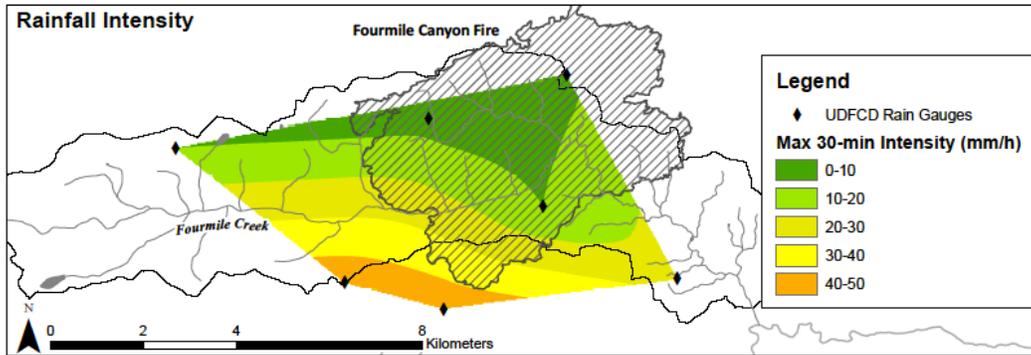
[Hydrography: USGS; Watershed: USGS StreamStats; Fire Perimeter: Boulder County GIS; Rainfall Gauges and Data: Urban Drainage and Flood Control District]

Rainfall
Average Amount: 17 mm
Average I_{30}: 22 mm/hr
Maximum I_{30}: 48 mm/hr
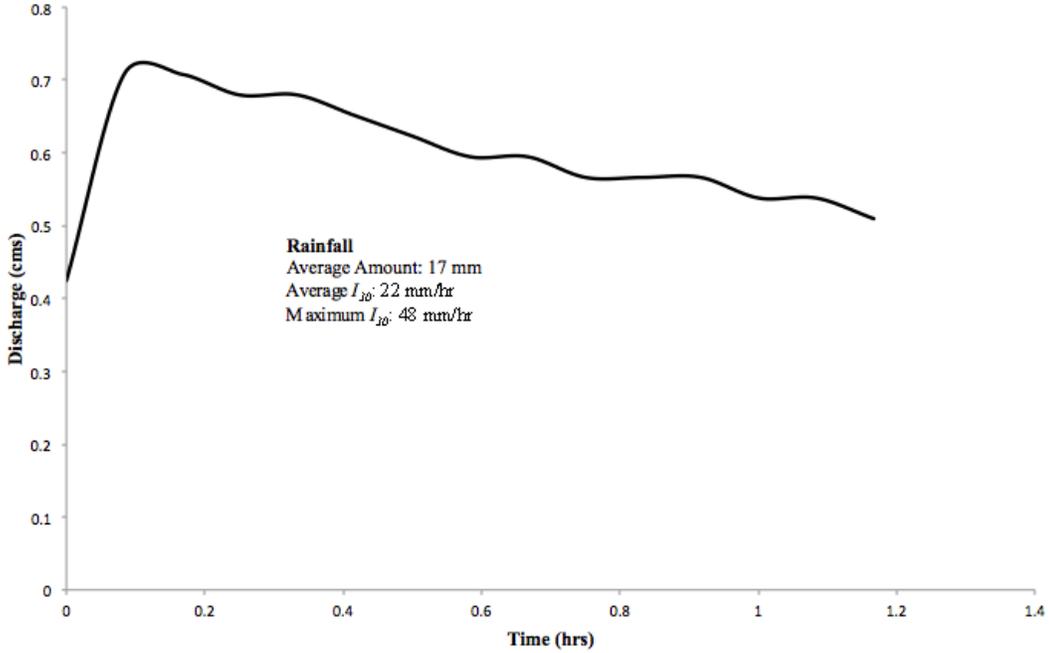
Figure 3.21. Lower rainfall but higher intensity event focused south of watershed on July 7, 2011 generates low peak discharge of 0.7 m^3/s.

July 13, 2011
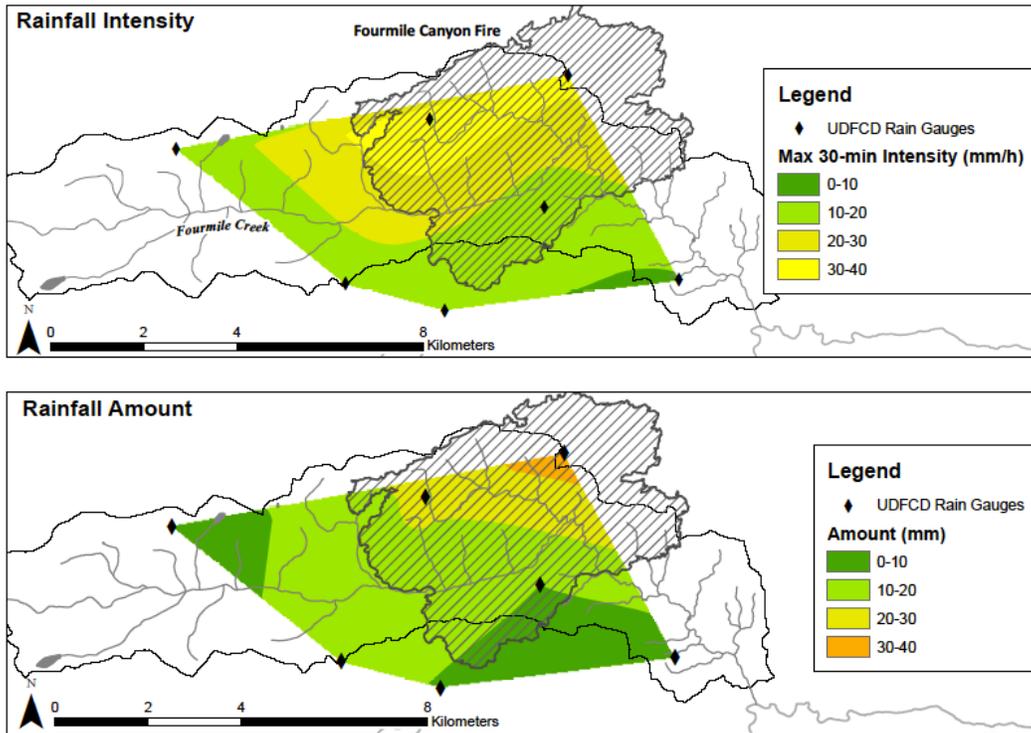
[Hydrography: USGS; Watershed: USGS StreamStats; Fire Perimeter: Boulder County GIS; Rainfall Gauges and Data: Urban Drainage and Flood Control District]

Rainfall
Average Amount: 14 mm
Average I_{30}: 19 mm/hr
Maximum I_{30}: 40 mm/hr
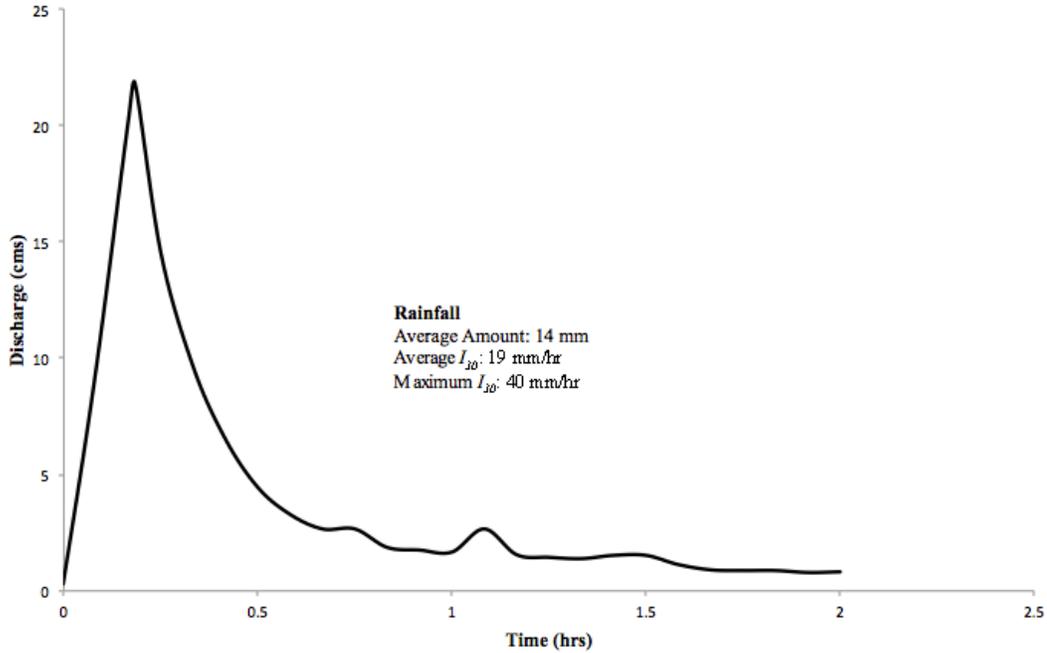
Figure 3.22. Moderate rainfall at high intensity focused on severely burned watershed, especially over Gold Run, on July 13, 2011 generates record peak discharge of 21.8 m^3/s.

July 5, 2012
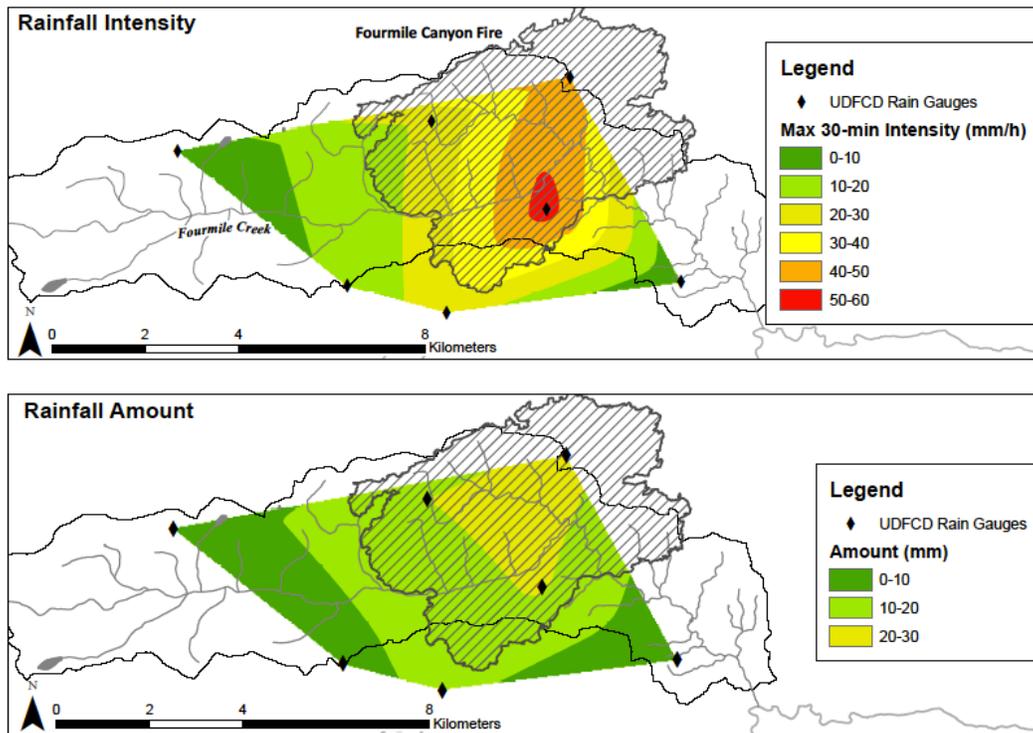
[Hydrography: USGS; Watershed: USGS StreamStats; Fire Perimeter: Boulder County GIS; Rainfall Gauges and Data: Urban Drainage and Flood Control District]
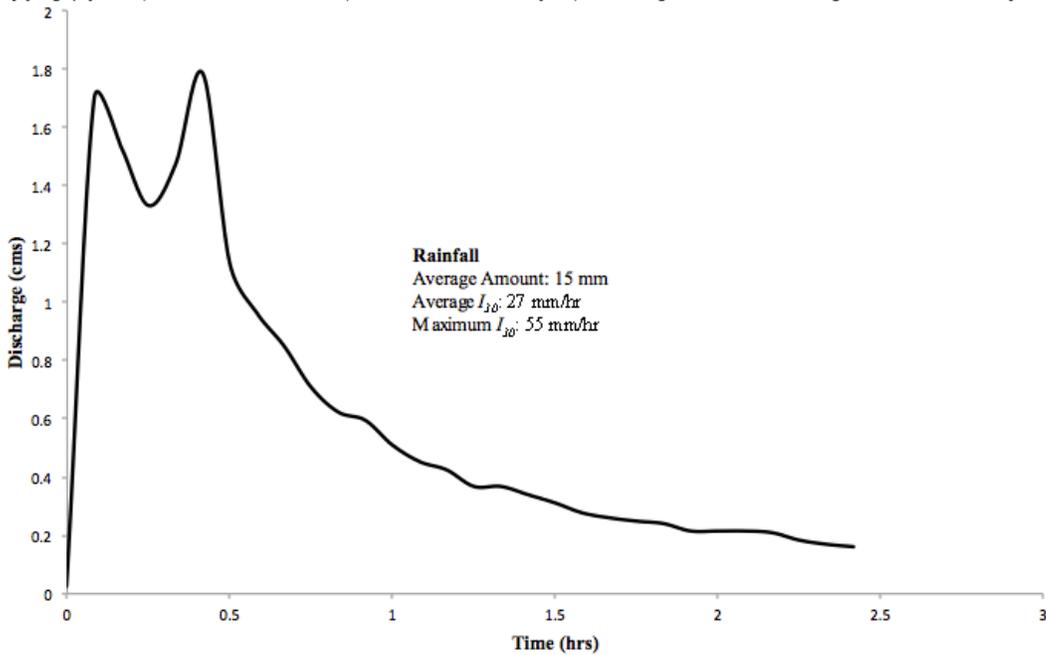
Figure 3.23. Moderate rainfall at high intensity over severely burned watershed on July 5, 2012 generates peak discharge of 1.8 m^3/s.

July 30, 2012
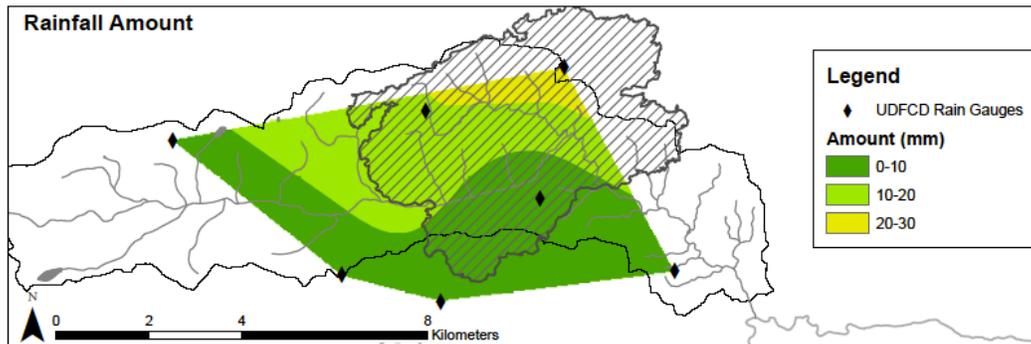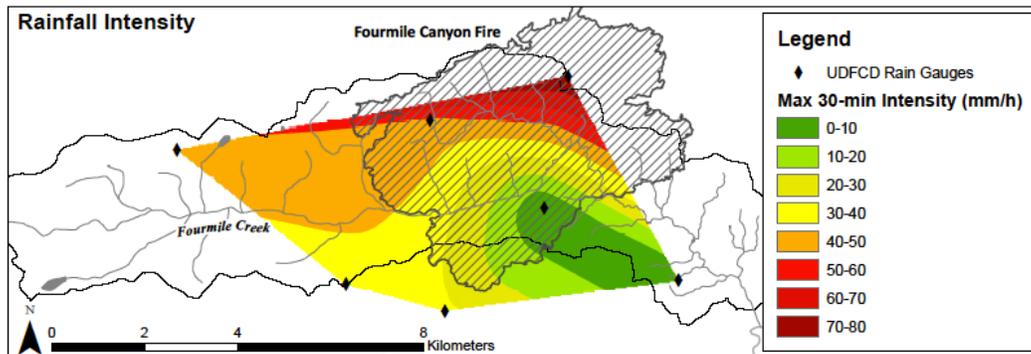
Rainfall Intensity

Fourmile Canyon Fire

Fourmile Creek

Legend
- ◆ UDFCD Rain Gauges

Max 30-min Intensity (mm/h)
- 0-10
- 10-20
- 20-30
- 30-40
- 40-50
- 50-60
- 60-70
- 70-80

0 2 4 8 Kilometers

Rainfall Amount

Legend
- ◆ UDFCD Rain Gauges

Amount (mm)
- 0-10
- 10-20
- 20-30

0 2 4 8 Kilometers

[Hydrography: USGS; Watershed: USGS StreamStats; Fire Perimeter: Boulder County GIS; Rainfall Gauges and Data: Urban Drainage and Flood Control District]

Rainfall
Average Amount: 14 mm
Average I_{30}: 48 mm/hr
Maximum I_{30}: 79 mm/hr
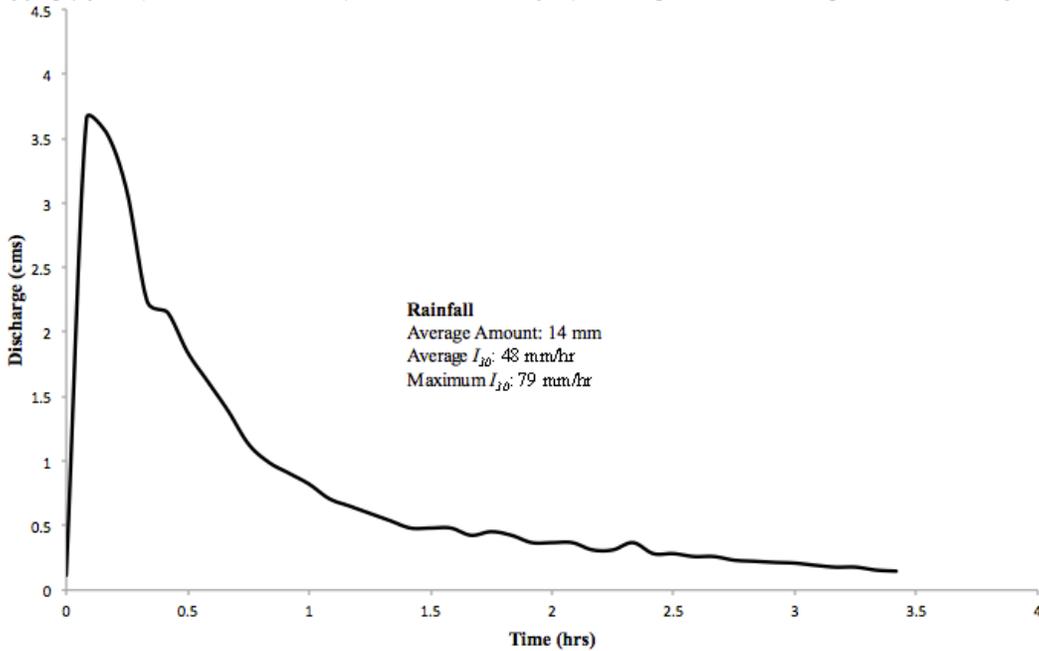
Figure 3.24. Moderate rainfall at very high intensity, especially over Gold Run, on July 30, 2012 generates peak discharge of only 3.7 m^3/s.

3.5. Sediment Composition, Shape, and Grain-size

Microscopic and laser grain-sizing techniques were employed to describe sediment samples to determine hillslope sediment contribution to sediment deposition in overbanks, gully deposits, and bedload samples on the valley floor. Samples observed under a binocular microscope revealed the prevalence of pyrogenic material in nearly all samples from all environments of deposition (Fig. 3.25). These charcoal pieces ranged in size from sub millimeter to several millimeters across. While apparent in nearly all samples, including the sampled ash deposits (Fig. 3.26), the abundance of charcoal was much greater in overbank and gully deposits compared with bedload samples. All non-ash samples were disintegrated grüs formed from the local granodiorite and include primarily mica, quartz, and feldspar, with some additional amphibole (Fig. 3.27). Most grains were angular to sub-angular indicating recent weathering from parent material.

Figure 3.25. Example of pyrogenic material found in majority of samples. Scale in millimeters.

Figure 3.26. Sampled ash deposit from severely burned north-facing hillslope. Note abundant pyrogenic and fine material. Scale in millimeters.

Figure 3.27. Typical channel or gully deposit from Fourmile Creek. Note abundant quartz and reflective mica flakes. All grains <150 μm.

Laser grain-size analysis of the <2 mm fraction of numerous hillslope, overbank deposit, and bedload samples yielded interesting results. Four bedload samples gathered from within and downstream of the burned area displayed increasing downstream mean diameters (Fig. 3.28). While errors in sampling cannot be eliminated from this result, a possible explanation may be in the winnowing of fine sediment from downstream bedload. This would be caused by the higher flows regularly experienced farther downstream rapidly flushing fine sediment, and thus coarsening the overall grain-size of downstream bedload relative to upstream bedload (Ryan *et al.*, 2011).
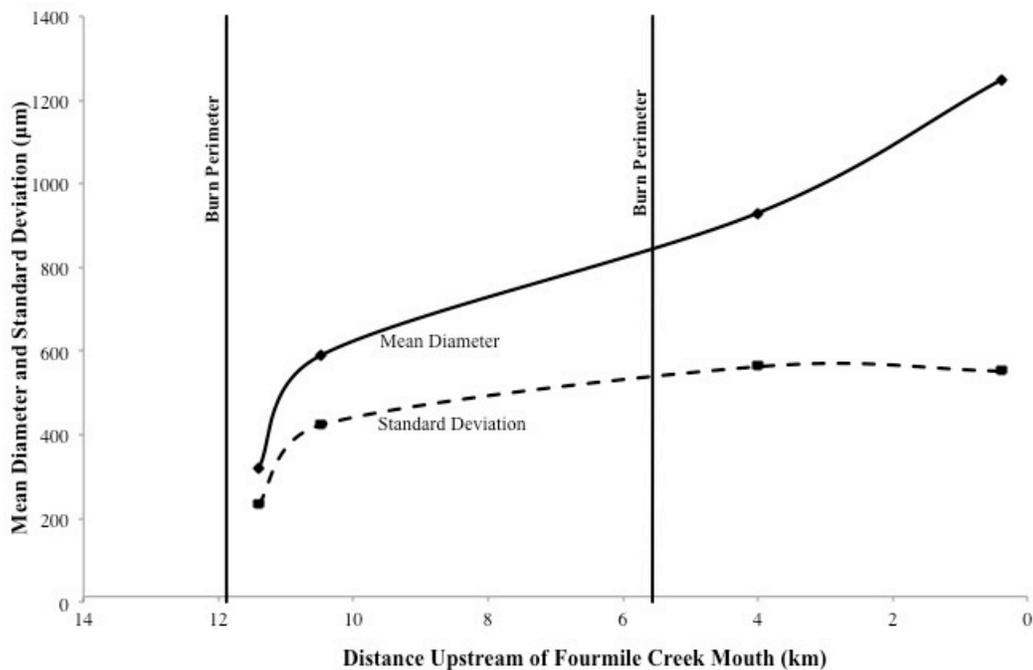
Figure 3.28. Increasing downstream mean diameter of bedload samples. Standard deviation remains relatively constant across samples.

The *in situ* hillslope ash deposit (Fig. 3.6) had a mean diameter of 75±55 μm. The mean diameter and distribution frequency of this ash is a close match with the 2011 overbank deposit sample, with a mean diameter of 72±48 μm (Fig. 3.29). On the

other hand, the mean diameter of the 2012 overbank deposit sample was 112±62 μm and the mean of the undisturbed upstream channel bank sample was 286±285 μm. Additionally, while the frequency distributions of the ash, 2011 deposits, and 2012 deposits appear to be bimodal, the channel bank deposits upstream of the burn area has a trimodal distribution (Fig 3.29).
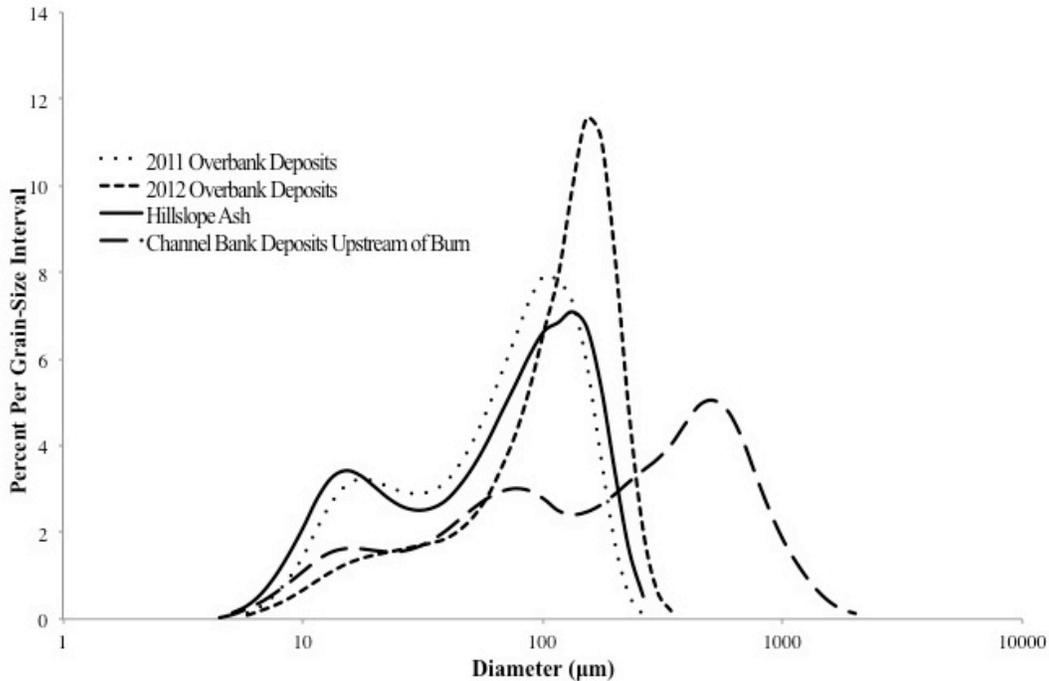
Figure 3.29. Frequency distribution comparison between ash, 2011 and 2012 overbank deposits, and upstream channel bank deposits. Note the close match in distribution between the 2011 and ash sample. Mean diameter increases in the 2012 overbank deposit and again in the upstream sample.

A trench in a large overbank deposit nearby the FCLM gauging station within the burned perimeter was analyzed for grain-size. This pit featured alternating sand and silt stratigraphy with a clay deposit near the bottom, which had a mean diameter of 8±3 μm (Fig 3.30). A burned grove of trees on a terrace just upstream of the pit appeared to contain an *in situ* ash deposit about 10 meters from the channel, which was also analyzed. The result for amalgamated sandy layers from the pit displayed a

mean diameter of 227±149 μm, whereas the silty layers displayed a mean diameter of

60±38 μm, similar to the upstream ash deposit, with its mean diameter of 64±54 μm

(Fig 3.31).

0-3 cm; intermittent fine sand and silt mix

3-4 cm; top most intermittent dark silty layer; abundant charcoal

4-16 cm; fine to medium sand; no apparent charcoal

16-18 cm; dark silty layer; abundant charcoal

18-23 cm; fine to medium sand; no apparent charcoal

23.5-38 cm; reddish clay layer; no charcoal

23-23.5 cm; very thin intermittent dark silty layer; abundant charcoal

38- cm; coarse sand; large cobbles; no charcoal

Figure 3.30. Pit sampled near eastern fire perimeter in overbank deposit. Note the alternating stratigraphy of sand and silt layers. Bottom of pit contains a coarse sand layer with abundant gravel and cobbles overlain by a reddish clay layer. Photo taken July 27, 2012 courtesy of W. Ouimet.
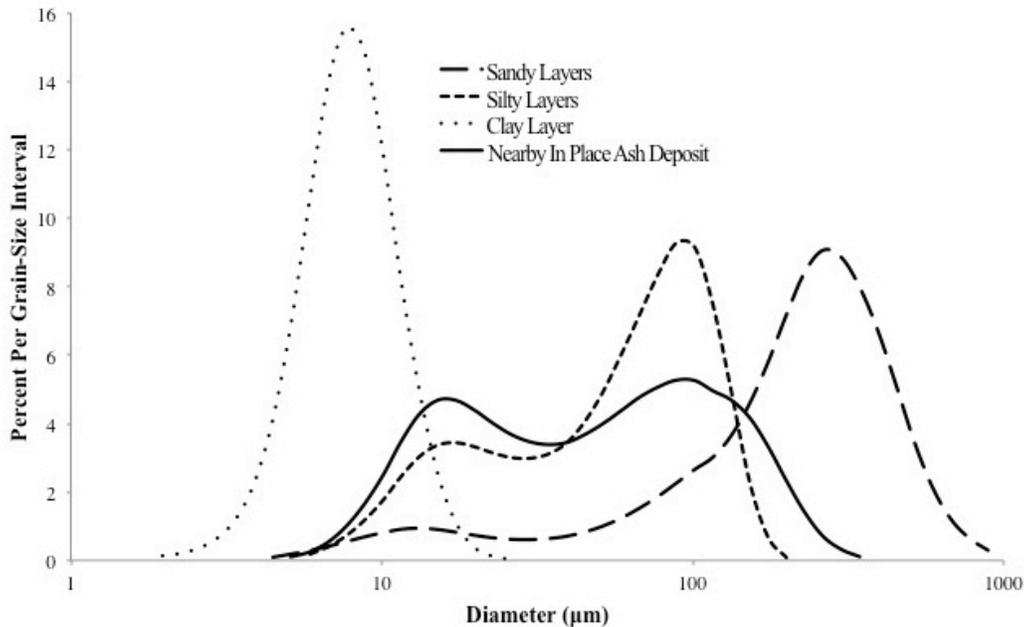
Figure 3.31. Frequency distribution for pit in Figure 3.30 and upstream *in situ* ash deposit. Note the difference in grain-size of each layer and the similar grain-size of the ash and silty layers.

3.6. Geochemical Analysis

3.6.1. Major Oxides

Overbank and channel bank deposits and ash samples were analyzed for major and trace elemental constituents to explore the effects of wildfire and mining on sediment chemistry. Additional analysis of Fourmile's water and sediment chemistry can be found in Beganskas (2012).

Major oxide results for 2011 and 2012 overbank deposits within and downstream of the fire area were compared with the channel bank deposits upstream of the fire area (Fig. 3.32). The results display decreased SiO_2 in the 2011 and 2012 disturbed area samples compared with the upstream sample. Conversely, Al_2O_3, Fe_2O_3, MgO, CaO, Na_2O, K_2O, TiO_2, and P_2O_5 all increased in the disturbed area samples compared with the upstream sample. MnO displayed no notable change in the downstream and upstream samples. The 2012 sample displays a slight return to upstream concentrations of SiO_2, compared with the 2011. All other major oxide concentrations are nearly identical between the 2011 and 2012 deposits.
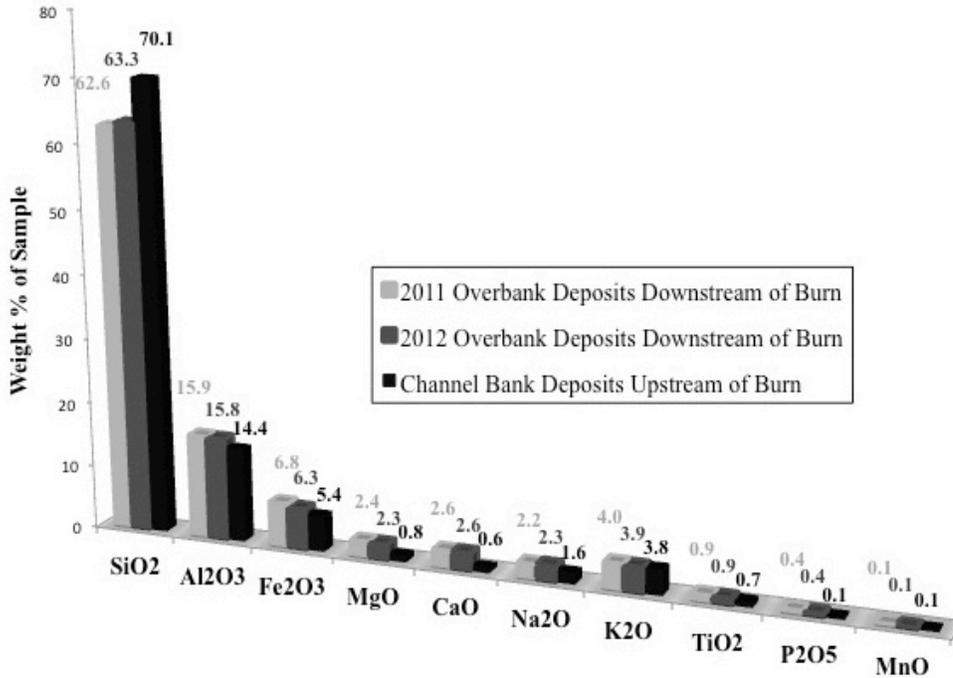
Figure 3.32. Major oxide comparison of three samples.

The results for major oxide analysis of the *in situ* hillslope ash sample are displayed in Table 3.7 for comparison with overbank deposit chemistry. MgO, CaO, and P_2O_5 concentrations in overbank deposits are shown as examples of downstream trends in major oxides in relation to the disturbed area, with all three displaying downstream increases, likely related to ash contribution (Fig. 3.33). Concentrations of these oxides fluctuate downstream of the disturbed area, but remain elevated against upstream concentrations.

Table 3.7. Major oxide concentrations of hillslope ash sample.

SiO_2 (wt %)	Al_2O_3 (wt %)	Fe_2O_3 (wt %)	MgO (wt %)	CaO (wt %)	Na_2O (wt %)	K_2O (wt %)	TiO_2 (wt %)	P_2O_5 (wt %)	MnO (wt %)
52.2	13.22	7.02	2.66	4.34	1.41	2.67	1.16	0.52	0.29
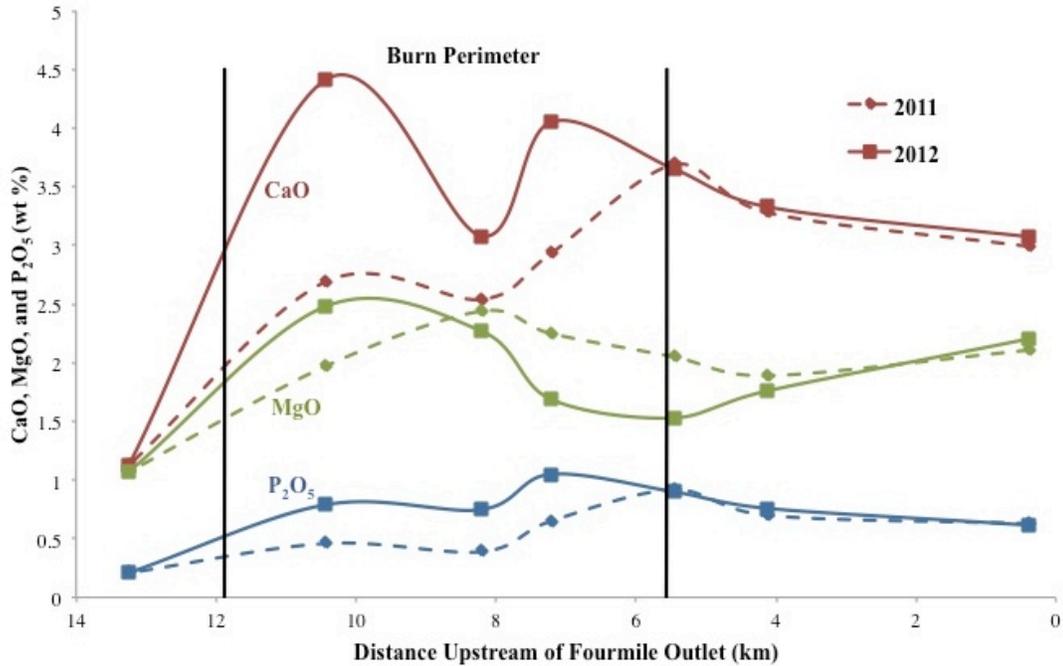
Figure 3.33. Downstream trends in some major oxides from overbank deposits. All increase in the disturbed area and remain elevated despite fluctuation. Hillslope ash concentrations of CaO, MgO, and P_2O_5 are 4.34, 2.66, and 0.52 wt % respectively.

3.6.2. Trace Elements

Trace elemental analysis revealed the effects of mining on sediment chemistry. Plots of gold, tungsten, zinc, and arsenic concentrations in 2011 and 2012 overbank deposits all spike downstream of the confluence of Gold Run and Fourmile Creek (Fig. 3.34–3.37). Excluding arsenic, all 2012 samples immediately downstream of Gold Run display elevated concentrations of these metals compared to the 2011 overbank samples. The results for each element in 2011 and 2012 overbank deposits from Gold Run just upstream of its outlet into Fourmile are also presented on each graph for comparison. As expected, excluding arsenic, the 2012 concentrations of these elements in the Gold Run overbank deposits are greater than the 2011 concentrations. The highest concentration of gold from any Fourmile deposit is 1029 ppb in the 2012 Gold Run overbank deposit sample (Fig. 3.34).

65
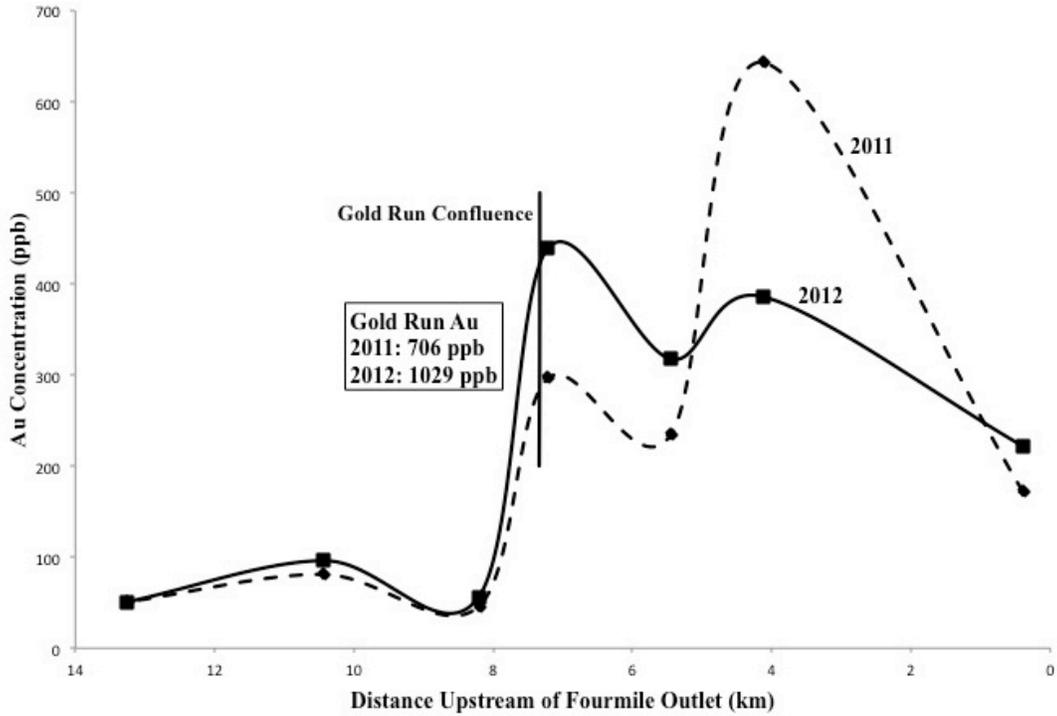
Figure 3.34. Downstream changes in gold concentration of overbank deposits. Note the large spike after Gold Run entrance and the high concentrations in the 2011 and 2012 Gold Run overbank deposits (inset box). 2012 concentration is higher than the 2011 concentration immediately downstream of Gold Run.
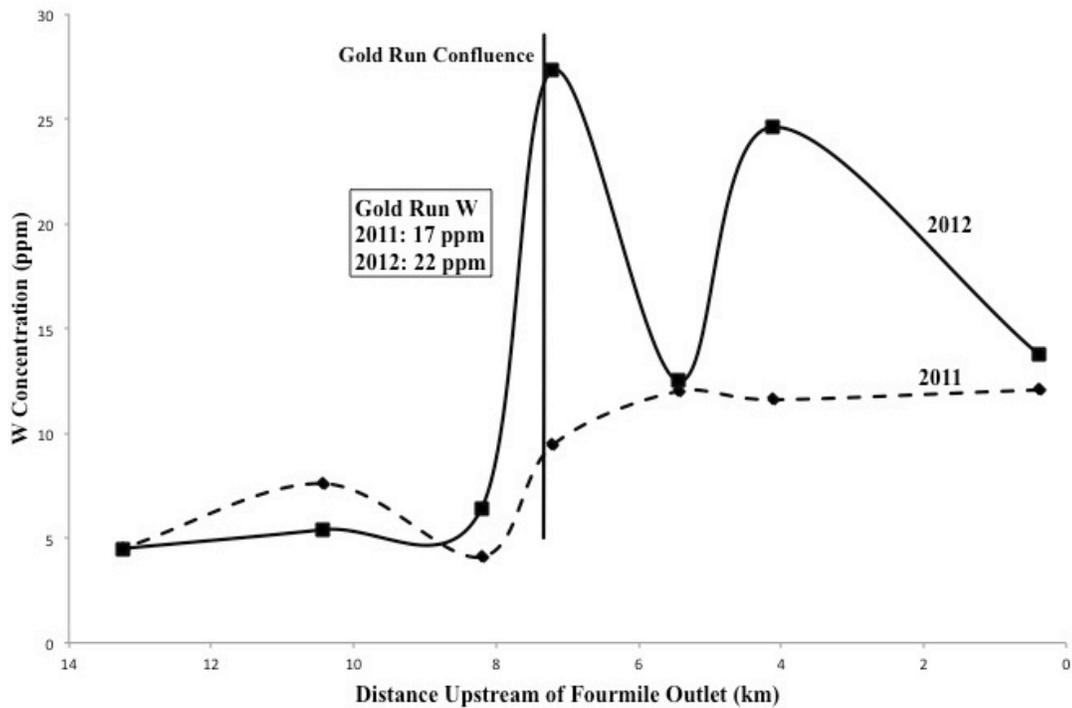
Figure 3.35. Downstream changes in tungsten concentration of overbank deposits. Same trends as those of gold concentrations in Figure 3.34.
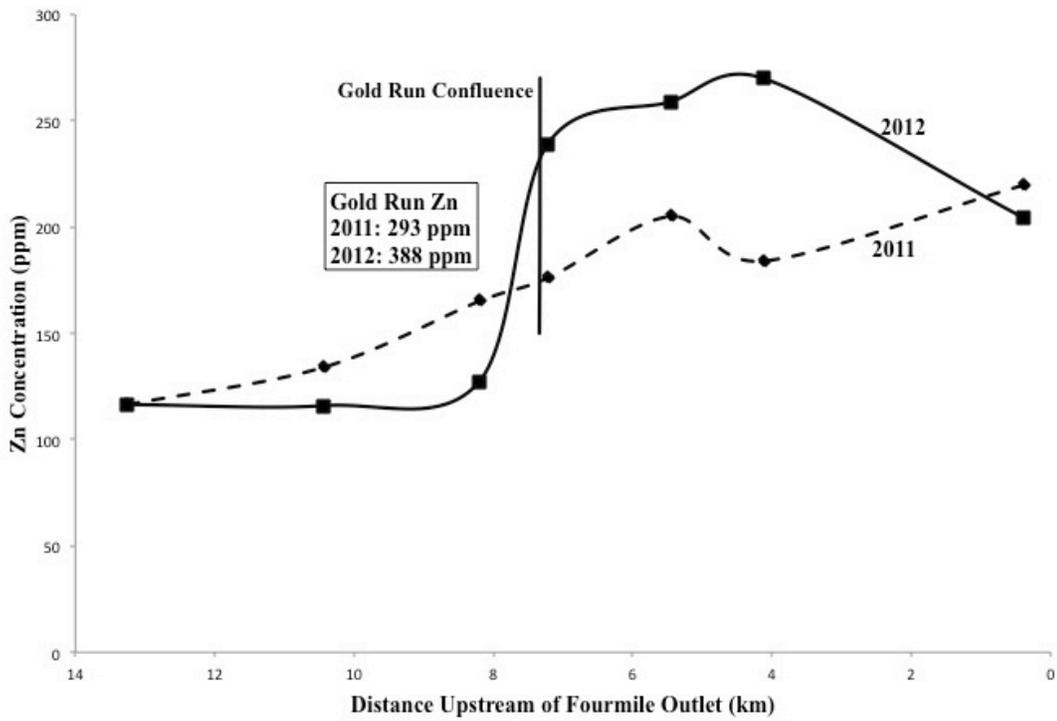
Figure 3.36. Downstream changes in zinc concentration of overbank deposits. Same trends as those of gold concentrations in Figure 3.34.
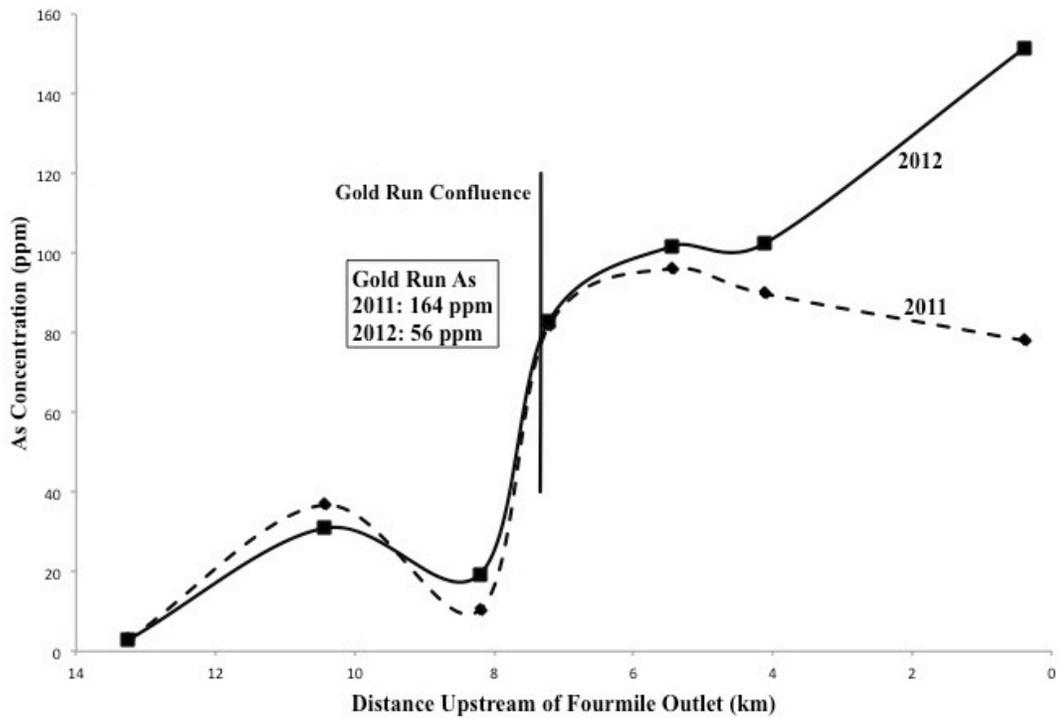
Figure 3.37. Downstream changes in arsenic concentration of overbank deposits. Same trends as those of gold concentrations shown in Figure 3.34, although 2012 samples are not elevated relative to 2011 samples.

In addition to these trace metals, lead and mercury were analyzed as potential sediment contaminants. These elements are plotted as a ratio to total organic carbon because of their high adherence to organic matter through biological uptake. Loss on ignition (LOI) measured as a weight percent loss after combustion at 550° C is used as a proxy for total organic carbon in this ratio. These plots indicate another downstream spike after the entrance of Gold Run (Fig. 3.38 & 3.39). However, this only appears to be the case in the 2012 samples and not the 2011, which display little change downstream of Gold Run. Furthermore, Pb:C and Hg:C ratios in the Gold Run overbank deposits do not appear to correlate with respective 2011 and 2012 ratios from Fourmile Creek overbank deposits downstream of Gold Run.
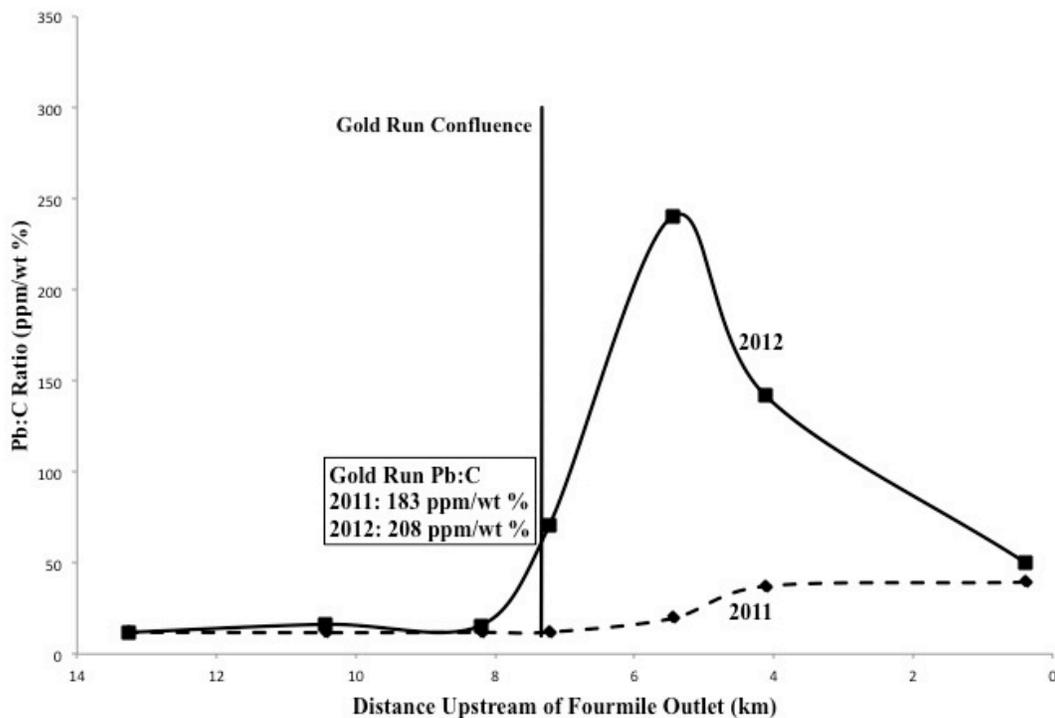
Figure 3.38. Downstream changes in Pb:C ratio of overbank deposits. A spike after Gold Run only appears in the 2012 deposits. Also, the Pb:C ratio of the 2012 Gold Run overbank deposit is only slightly greater than the 2011 ratio.
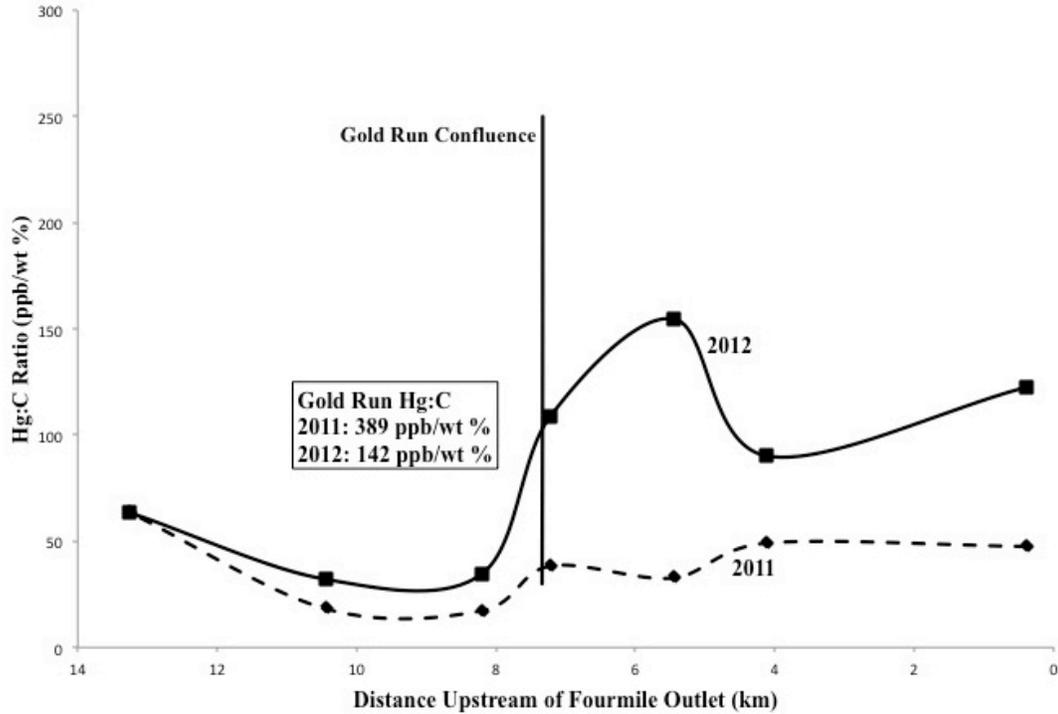
Figure 3.39. Downstream changes in Hg:C ratio of overbank deposits. A spike after Gold Run only appears in the 2012 deposits, however the Hg:C ratio of the 2011 Gold Run overbank deposit is actually greater than the 2012 ratio.

3.6.3. Radionuclides

The near-surface radionuclide activity of an undisturbed hillslope transect from nearby Gordon Gulch is shown in Figure 3.40. The highest measured activity of ^{137}Cs and ^{210}Pb from Gordon Gulch is approximately 50 Becquerels/kg (Bq/kg) and 180 Bq/kg respectively, as measured at the toeslope. In contrast, the highest measured activity of ^{137}Cs and ^{210}Pb of 113 Bq/kg and 355 Bq/kg respectively are found in the *in situ* hillslope ash deposit from Fourmile Canyon, roughly double the undisturbed maximum (Table 3.8). Ash transported downslope and ponded behind a tree root and the *in situ* ash sample from nearby the FCLM gauging station on the valley floor display radionuclide activities within the range of measurements from Gordon Gulch.

69
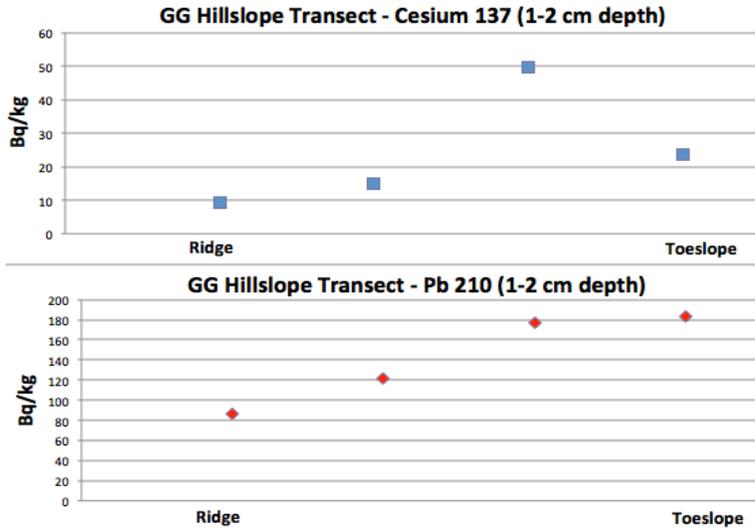
Figure 3.40. Radionuclide activity for an undisturbed hillslope transect in Gordon Gulch. Figure courtesy of W. Ouimet.

Sample	^{137}Cs Activity (Bq/kg)	^{210}Pb Activity (Bq/kg)
In situ hillslope ash (Fourmile)	**113**	**355**
Eroded hillslope ash (Fourmile)	66	151
In situ floodplain ash (Fourmile)	17.5	179
Undisturbed toeslope (Gordon Gulch)	**50**	**180**

Table 3.8. Radionuclide activity results for ash samples from Fourmile Canyon compared with undisturbed Gordon Gulch hillslope samples in Figure 3.40.

Radionuclide activities for the 2011 and 2012 overbank samples are compared to the measured activity in the upstream channel bank sample in Table 3.9. There is a clear trend exhibited in this data with the highest measured activity of ^{137}Cs and ^{210}Pb found in the 2011 sample (36 Bq/kg and 144 Bq/kg respectively). While this activity is comparable to undisturbed samples (Fig. 3.40), this result likely represents the contribution of hillslope ash to these deposits, given the reduced radionuclide activity in the upstream and 2012 samples.

Sample	^{137}Cs Activity (Bq/kg)	^{210}Pb Activity (Bq/kg)
2011 overbank deposits	36	144
2012 overbank deposits	13	88
Upstream channel bank deposits	4	98

Table 3.9. Radionuclide activity results for overbank deposits from within and downstream of the fire area and channel bank deposits upstream of the fire

Selected layers from the overbank pit stratigraphy in Figure 3.30 were also run for ^{137}Cs and ^{210}Pb (Table 3.10). The focus here was on the silty layers, as grain-size and microscopic results suggest that these deposits contain the greatest ash contribution. While no clear trend in activity is observable, these results do confirm that ash and combusted organic matter is a key component to these deposits, which are likely derived from burned hillslopes. This is especially clear in the very high activity of ^{210}Pb in all silty deposits, one of which from near the top of the pit has the highest measured activity of 567 Bq/kg. The clay layer underlying all of these deposits has radionuclide activities comparable with the upstream undisturbed channel bank deposits (Table 3.9), indicating its prefire–and likely pre-atmospheric nuclear testing–origin.

Sample	^{137}Cs Activity (Bq/kg)	^{210}Pb Activity (Bq/kg)
Top silty deposit from July 30, 2012 event	53	298
3-4 cm silty deposit	130	567
16-18 cm silty deposit	93	396
23-23.5 cm silty deposit	50	248
23.5-38 cm clay deposit	**2.5**	**104**

Table 3.10. Radionuclide activity results for stratigraphy of sampled pit in Figure 3.30

4. Discussion

4.1. Hydrologic Changes

Ephemeral postfire increases in runoff and discharge account for increased sediment delivery and deposition, and thus the long-term impact of the 2010 Fourmile Canyon Fire. Comparison of peak postfire flows to large prefire discharge events is hindered by a lack of significant floods in the prefire instantaneous record (1987–1994), excluding the June 1991 rain-on-snow event. Above average precipitation in July 2011 and 2012 for Boulder, evident in heightened postfire July mean discharge (Fig. 3.12), may be responsible for the higher frequency of postfire discharge events (High Plains Regional Climate Center, 2012). Despite this caveat, the large magnitude of the postfire peaks and the scarcity of notable prefire discharge events through the seven-year prefire instantaneous record are telling of the impressive effect of wildfire on large-scale hydrologic changes.

Results unexpectedly display a reduction in postfire mean daily flow versus prefire values (Fig. 3.13 & Table 3.2). This could be related to a lack of postfire data in generating an accurate flow duration curve, or below average snowmelt in Spring 2012 decreasing baseflow (USGS Surface-Water, 2012). Another possibility is that increased watershed flashiness would allow for high, short duration peaks while maintaining low mean daily discharge possibly caused by high infiltration in coarse soils and increased evaporation of rainfall on severely burned, barren slopes.

The shortened time base of postfire hydrographs and their reduced time to rise indicate the rapid travel time of runoff from burned slopes to Fourmile Creek (Tables 3.3 & 3.4). Furthermore, dual peaks found in seven of the prefire hydrographs

indicate a lagged runoff response in this long, narrow watershed. This may be caused by watershed shape, variable rainfall, or by relative timing of discharge in Fourmile's headwaters and Gold Run's drainage. In either case, the change in hydrograph shape in the postfire record indicates the watershed's flashier nature (Fig. 3.18).

Low effective rainfall values indicate that even within hyper-dry hydrophobic soils of the burned area infiltration remains high in these gravelly sandy loam soils (Table 3.6). Evaporation of potential runoff, caused by the removal of canopy during the fire and exposure of bare slopes to intense sunlight, likely has a great influence over miniscule effective rainfall values. This is especially significant on north-facing slopes, which tend to have denser stands of Douglas fir and Limber Pine prior to the fire than the sparser ponderosa pine-dominated south-facing slopes.

4.2. Postfire Flooding, Sediment Delivery, and Recovery

Intense rainfall over severely burned slopes soon after wildfire is necessary for significant discharge and erosion. The catastrophic July 13, 2011 flood, followed just a year later by intensified rainfall but order of magnitude reduction in unit-area peak discharge on July 30, 2012, indicates the need for flood precautions until the first significant rainfall event after wildfire. The high frequency of the rain events capable of generating these unprecedented floods is difficult to combat. Mulching on severely burned slopes has been demonstrated to be somewhat effective at reducing these flows, yet mulching carried out in Fourmile Canyon in the months following the fire did not prevent the 70-year flood event (Boulder County Flood Mitigation & Land Rehabilitation, 2012).

The rapid, peaked response of postfire discharge observed in these floods is caused by decreased interception and evapotranspiration of foliage and groundcover along with reduced infiltration of hydrophobic soils creating low energy flow paths for runoff on steep slopes. These factors magnify the effect of low recurrence interval rain events (maximum 5 years).

The observed return of grasses and the likely elimination of soil hydrophobicity (Huffman *et al.*, 2001; Moody and Ebel, 2012) will lead to additional recovery of the watershed to prefire hydrologic conditions in the upcoming summer. Furthermore, the sparse presence of remaining hillslope fine deposits–ash–would suggest that additional yield will be limited and that surface stone lag is reducing hillslope erosion (Fig. 3.4 & 3.5). An immediate postfire peak in discharge and sediment yield followed by a rapid decline agrees with other postfire studies (e.g. Moody and Martin, 2001a; Benavides-Solorio and MacDonald, 2005; Reneau *et al.*, 2007).

The deposition of sediment on the valley floor from two summers of rainfall-runoff events led to fire-associated channel bank storage of approximately 19,000 t. This omits significant contributions from recent gully fan deposits, Gold Run's drainage, anthropogenic removal, and throughput. Inclusion of these factors accounts for the discrepancy with the estimated 39,400 t two-year sediment yield, which is in close agreement with the potential delivery predicted by Ruddy *et al.* (2010). Field evidence shows that this sediment was derived entirely from within the burned area.

The angularity of the grüs in finer overbank and coarser bedload samples displays the freshness of sediment, as stream transport has not caused rounding of

these clasts. This indicates the typically rapid transport of sediment from Fourmile

Canyon into the larger Boulder Creek Watershed. In the future, moderate rainfall

events will be capable of remobilizing near-channel sediment deposits, flushing them

out to Boulder Creek, and maintaining a constant rate of basin sediment yield for

decades despite the reduction in upland erosion (Trimble, 2009). However, as many

of the recent deposits lie some distance from the channel, it is likely that they will

become persistent landscape features, requiring large magnitude rare rainfall and

flood events for removal. The legacy of sediment influx from the fire could persist for

several decades given the swift hydrologic recovery of Fourmile Canyon.

4.3. Mining Legacy

The persistence of fire-associated sediment deposits becomes a potential issue

for water quality in Fourmile Creek in light of trace metal contamination from

historical mining activity in Fourmile Canyon.

Gold Run is the primary contributor of metals to Fourmile Creek as evidenced

by the spike in concentration immediately downstream of this tributary's outlet (Fig.

3.34–3.39). This is logical as Gold Hill was the locus of mining activity within

Fourmile Canyon (Fig. 1.7; Twitty, 2007). The increased concentrations of Au, W,

and Zn in 2012 versus 2011 deposits (Fig. 3.34–3.36) could indicate increased

downstream transport of trace metals from tailings piles within Gold Run's drainage

in the second summer after wildfire. It is unknown whether this trend will continue,

or if the return of vegetation will curtail erosion of mine tailings in the future. The

lack of a 2011 spike in Fourmile overbank deposits for Pb:C and Hg:C (Fig. 3.38 &

3.39) may be explained by greater LOI values in the 2011 deposits (average 3.98 wt

%) compared with 2012 deposits (average 1.64 wt %). This reflects the heightened organic C input in 2011 with the initial stripping of burned slopes.

As discussed, storage of fire-associated sediment deposits in the absence of large flood events will likely lead to lengthy residence times. Based on the number of tailings piles throughout this drainage, elevated concentrations of trace metals will persist in Fourmile sediments for many decades, perhaps even centuries. While fire-associated flood events are capable of flushing contaminated sediment from the system, the input of additional sediment from tailings piles will cause little net change in trace metal concentrations (Marcus *et al.*, 2001). Although there is no evidence of worrisome water concentrations of these elements (Writer and Murphy, 2012), their presence in sediment deposits throughout Fourmile Canyon signifies a need for continual monitoring.

4.4. Sediment Source

Sediment source tracing was attempted to determine the significance of hillslope erosion to recent deposits in the valley of Fourmile Canyon. Grain-size, major oxide, and radionuclide results indicate the contribution of hillslope sediment–primarily ash–to overbank deposits. Based on this contribution, it is evident that burned hillslopes underwent substantial denudation following the runoff events of the past two years.

4.4.1. Grain-size

The mean diameters of the *in situ* hillslope ash and *in situ* floodplain ash agree closely with the previously reported mean diameter of ponderosa pine ash of 59±10

μm (Bookter, 2006). Combined with the close match in frequency distribution between the ash and 2011 overbank deposits (Fig. 3.29), this result appears to indicate that ash delivery dominated during the July 13, 2011 flood that created these deposits. Furthermore, the increased grain-size distribution of the 2012 overbank sample indicates a decrease in ash presence following rapid stripping in 2011. The frequency distribution of the upstream channel bank samples may represent the background undisturbed grain-size of near-channel deposits along Fourmile Creek.

4.4.2. Major Oxides

The combustion of organic matter during wildfire leads to mineralization of major nutrients and the entrainment of these oxides on ash deposits (Certini, 2005). Higher concentrations of SiO_2 in undisturbed sediments are probably a result of greater amounts of grüs, and thus quartz, associated with the weathering of granodiorite outcrops. This SiO_2 concentration is obscured in deposits from the disturbed area by hillslope delivery of ash rich in mineralized organic matter (Fig. 3.32). This ash is responsible for the increase in oxides of organic matter nutrients as illustrated by the downstream trends in MgO, CaO, and P_2O_5 (Fig. 3.33).

The USGS reports increased concentrations of Mn, Al, and Fe in Fourmile water chemistry the summer following the wildfire (Writer and Murphy, 2012). Soluble MnO entrained on ash likely causes increased Mn concentrations (Gonzalez Parra *et al.*, 1996; Ice *et al.*, 2004). Overbank concentrations of MnO from the disturbed area are within the range of 0.12–0.18 wt %, but hillslope ash concentrations are measured at 0.29 wt %. This indicates the potentially detrimental effect of stream water nutrient loading through ashes rich in soluble oxides. On the

other hand, Fe_2O_3 and Al_2O_3 are elevated in disturbed overbank deposits relative to upstream deposits (Fig. 3.32), but only Fe_2O_3 is elevated in the ash at 7.02 wt % relative to the upstream sample at 5.4 wt %. Al_2O_3 is actually lower in the ash at 13.22 wt % compared with the upstream value of 14.4 wt %. Nutrient influxes associated with the Fourmile Fire are responsible for increased stream biofilm but are not currently a concern for water quality (Writer and Murphy, 2012; Writer *et al.*, 2012).

4.4.3. Radionuclides

Radionuclide loading in organic matter and subsequent deposition on fine mineral matter during combustion is responsible for the increased activity of ^{137}Cs and ^{210}Pb of *in situ* hillslope ash from Fourmile Canyon (Table 3.8; Wilkinson *et al.*, 2009). The lack of elevated radionuclide activity in eroded and *in situ* floodplain ash may be a result of additional, non-ash sediment diluting the radioactivity of these deposits. Radionuclide activities of valley floor deposits appear to confirm the rapid stripping of ash in 2011, with limited contribution to the 2012 deposits (Table 3.9). Mineral matter dilution is likely responsible for the relatively low activities measured in these overbank deposits. The activity of the upstream sample may indicate typical background channel bank radionuclide activity in Fourmile.

The silty deposits from the pit stratigraphy (Fig. 3.30 & Table 3.10) display elevated activity of ^{137}Cs and ^{210}Pb, indicating the adherence of these radionuclides to organics and fine material (Reneau *et al.*, 2007). In conjunction with grain-size results, radionuclides indicate that a significant portion of this fine stratigraphy is fire-associated ash. Furthermore, the clay layer at the base of this stratigraphy displays no

elevated radionuclide activity, indicating that this deposit is likely pre-atmospheric nuclear testing in origin (*c.* 1950s; W. Ouimet, personal communication). Therefore, the sediment overlying this (~23 cm) is likely entirely recent fire-flooding related deposition.

4.5. Geomorphic Significance of Wildfire

Field observations of recent depositional features and sediment source tracing results indicate the large contribution of burned hillslope regolith to valley floor deposits downstream of the western fire perimeter in Fourmile Canyon. The estimated 39,400 t fire-associated sediment yield brought by summer flooding allows for discussion of the potential long-term geomorphic impacts on this Front Range catchment. Back-calculating from the deposit density (~1.7 t/m^3), this represents a depth of 1.6 mm within the burned area (14.5 km^2). However, this is the average denudation, as erosion was much greater on high-severity burned slopes. If low and moderately burned areas are taken as a minimal part of total yield, then the volume extrapolated over the high-severity burned area (2.5 km^2) represents 9 mm of denudation. Assuming that the majority of sediment delivery occurred following the July 13, 2011 storm, it is possible to generate return periods for denudation associated with similar fire-flood events.

Elliot and Parker (2001) present a method for calculating the return period of large postfire floods as the combination of three probabilities: (1) The return period for severe fires (P_F), (2) the return period for the rainfall event that generated the flood (P_P), and (3) the probability of said rain event occurring while hillslopes are

susceptible to severe erosion (P_S). The recurrence interval for the fire-flood event (RI_{FF}) may then be taken as:

$$RI_{FF} = \frac{1}{P_F \cdot P_P \cdot P_S}$$

The return period for severe wildfire is approximately 60 years for a given location in the Front Range (Kaufmann *et al.*, 2000). Fire scar evidence in Fourmile Canyon indicates two previous severe fires in 1860 and 1894, and none thereafter until the 2010 Fourmile Fire (Schoennagel, 2010). This is consistent with a decline in severe fire frequency observed since the onset of anthropogenic fire suppression in the early 1900s (MacDonald and Stednick, 2003). The increasing frequency of severe wildfire in the Western US has the potential to lower the return period (increase the probability) further (Westerling *et al.*, 2006). Based on this, three estimates of severe fire return periods are assessed: 40-year ($P_{F1}={}^1/_{40}$), 60-year ($P_{F2}={}^1/_{60}$), and 100-year ($P_{F3}={}^1/_{100}$).

The return period of the rain event that generated the 2011 70-year flood was two years ($P_P=0.5$). Elliot and Parker (2001) assume that the chance of a 1-hour, 5-year rain event capable of significant erosion soon after fire is 50% ($P_{S1}=0.5$). Assuming that the high frequency of the July 13, 2011 rain event would raise its chance of occurrence while hillslopes are still vulnerable to erosion, an 80% chance of rain soon after the fire is also examined ($P_{S2}=0.8$). This is reasonable as this rainstorm occurred nearly one year after the fire but still generated the observed discharge; even with other June and early July rain events preceding it. It is conceivable that this event could have occurred even later, in the absence of other notable storms, and still have generated large-scale erosion.

The joint probabilities used to calculate these fire-flood recurrence intervals (Table 4.1) describe the interaction between processes that are not well defined probabilistically (Elliot and Parker, 2001). A wide range of possible values exists for fire-flood recurrence given the length of time to hillslope recovery and the spatiotemporal variability in burning and convective rain storms.

Table 4.1. Recurrence interval of fire-flood events given a constant P_P=0.5, P_{S1}=0.5, and P_{S2}=0.8.

Return Period for Fire (P_F)	Recurrence Interval for Fire-Flood Event with P_S=0.5 (yrs)	Recurrence Interval for Fire-Flood Event with P_S=0.8 (yrs)
$^1/_{40}$	160	100
$^1/_{60}$	235	150
$^1/_{100}$	400	250

Despite uncertainty, the denudation caused by the 2010/2011 Fourmile Fire-Flood event can be extrapolated to thousand and million year time scales given these recurrence intervals. The 1.6 mm average denudation for the entire burned area is extrapolated in Table 4.2. However, field observation of localized sediment deposits below high-severity burned slopes suggests that the vast majority of erosion occurs in these areas. It is therefore assumed that 9 mm of denudation constrained to the high-severity burned slopes best represents the impact of fire-flood disturbances on these landscapes (Table 4.3).

Table 4.2. Long-term denudation rates based on fire-flood recurrence averaging denudation over the entire burned area (14.5 km^2) of 1.6 mm.

Recurrence Interval for Fire-Flood Event (yrs)	Potential Denudation Rate (m/kyr)	Potential Denudation Rate (m/Myr)
50% chance of rainfall prior to hillslope recovery:		
160	0.01	10
235	0.007	7
400	0.004	4
80% chance of rainfall prior to hillslope recovery:		
100	0.016	16
150	0.011	11
250	0.006	6

Table 4.3. Long-term denudation rates based on fire-flood recurrence assuming a localized denudation only on high-severity burned area (2.5 km^2) of 9 mm.

Recurrence Interval for Fire-Flood Event (yrs)	Potential Denudation Rate (m/kyr)	Potential Denudation Rate (m/Myr)
50% chance of rainfall prior to hillslope recovery:		
160	0.06	60
235	0.04	40
400	0.02	20
80% chance of rainfall prior to hillslope recovery:		
100	0.09	90
150	0.06	60
250	0.04	40

To put these rates in perspective, an approximate background erosion rate of 55 m/Myr for basins in Fourmile Canyon is reported from cosmogenic radionuclides averaging the last 15–20 ka (W. Ouimet, personal communication). Long-term extrapolation of average denudation over the entire burned area presents a 10–30% potential contribution to long-term erosion (Table 4.2). Restricting significant erosion to the high-severity burned area suggests a much greater significance (Table 4.3). Even the greatest estimate of fire-flood recurrence (400 years) displays a 40%

contribution to long-term erosion (20 m/Myr). Increasing fire frequency expected with climate change has the potential to raise this contribution to 105–170% of long-term denudation (60–90 m/Myr) depending on the occurrence of significant rainfall prior to hillslope recovery.

Recurrence intervals and sediment yield used to extrapolate long-term impacts rely on a number of restrictive assumptions. Taken as best estimates, the results indicate the significance of infrequent wildfire and flooding on erosion in the West, confirming the original hypothesis of Swanson (1981). Furthermore, it is likely that this influence will increase with anthropogenically induced climatic forcing increasing fire frequency. Doubling of long-term erosion rates in a warmer climate is feasible assuming that the generation of available sediment by bedrock weathering can keep pace.

5. <u>Conclusions</u>

The growing field of wildfire research still has many questions to answer. Establishing better links between burn severity and hydrologic implications is perhaps the most important component in predicting landscape effects of heterogeneous fire patterns. Important to wildfire studies is baseline prefire data on discharge, rainfall, infiltration, runoff, and sediment yield. This is a tall order given the unpredictability of wildfire occurrence, and relies on the serendipitous conjunction of wildfire with long-term study sites. That said the results of this and other similar studies aid our understanding of the immediate effect of wildfire, which can lead to better predictive efforts and damage mitigation techniques. Such efforts are essential with arid conditions related to climate change increasing severe fire frequency (Healy, 2013).

The 2010 Fourmile Canyon Fire is an excellent example of the geochemical, hydrological, and geomorphological effects of wildfire. This study site is important given its proximity to the populous city of Boulder and the canyon's early mining history. Both the immediate and long-term impacts of this fire concern those living in and around Fourmile Canyon. These impacts are manifested in destructive floods–a short-lived concern in even the most severely burned areas as hydrophobic soil recovery and revegetation reduces runoff within a few years.

The more subtle geochemical and water quality impacts of nutrient loading, suspended sediment increases, and the delivery of sediment contaminated with trace metals from historical mining activity are much longer-term concerns in Fourmile Canyon. Although hydrologic recovery is swift, the legacy of sediment associated with flooding is enduring. Where sediment is uncontaminated and the population is

scarce, this sediment influx is not a concern to people, but this is not the case in Fourmile Canyon. The short relaxation time of elevated runoff and sediment yield leads to long residence times of geomorphic features (overbank and gully alluvial fan deposits) created soon after the fire (Moody and Martin, 2001a). While the geochemical impact of ash input appears to be minimal, many of these features likely contain appreciably elevated contaminants linked with mining. Geochemical results indicating the influence of mining and wildfire are in agreement with the previous study of Fourmile water and sediment chemistry (Beganskas, 2012).

The long-term geomorphic impact of fire-flood events is not well constrained, but is likely significant. The erosional and depositional features observed in July 2012 indicate the importance of such events to hillslope denudation, sediment delivery to channel networks, and the contribution of this sediment influx to channel morphology (Legleiter *et al.*, 2003). Approximations of sediment yield from detailed field measurement and recurrence estimates of fire-flood events can provide some insight into the potential long-term contribution of wildfire to erosion; however, a range of possibility exists when working with many assumptions, which are often educated guesses. Where the hydrologic and geochemical results of this study are definitive, the geomorphic impact of wildfire is apparent qualitatively and more difficult to define quantitatively, besides to say that its influence is sure to increase with greater fire frequency associated with climate change (Westerling *et al.*, 2006).

6. <u>References</u>

Beganskas, S., 2012, The Geochemical Impact of Wildfire and Mining on the Fourmile Creek Watershed, Colorado [Honors Thesis]: Massachusets, Amherst College, 132 p.

Bell, F.G., and Donnelly, L.J., 2006, Mining and its Impact on the Environment: New York, Taylor & Francis.

Benavides-Solorio, J.D., and MacDonald, L.H., 2005, Measurement and prediction of post-fire erosion at the hillslope scale, Colorado Front Range: International Journal of Wildland Fire, v. 14, p. 1–18.

Biswas, A., Blum, J.D., Klaue, B., and Keeler, G.J., 2007, The release of mercury from Rocky Mountain forest fires: Global Biogeochemical Cycles, 21 p.

Bookter, A., 2006, Erosional Processes After Wildfires: The Impact of Vegetative Ash and the Morphology of Debris Flows [Masters Thesis]: Montana, University of Montana, 69 p.

Boulder County, 2012, Flood Mitigation & Land Rehabilitation: http://www.bouldercounty.org/property/forest/pages/4milefirelandrehab.aspx (accessed Nov. 2012).

Boulder County, 2012, GIS Downloadable Data: http://www.bouldercounty.org/gov/data/pages/gisdldata.aspx (burn severity and fire perimeter for Fourmile Fire accessed Oct. 2012).

Bradley, H.A., 2008, Sediment chemistry and benthic macro-invertebrate communities within an acid mine drainage impacted stream: Earth & Environment, v. 3, p. 1–31.

Cannon, S.H., Bigio, E.R., and Mine, E., 2001, A process for fire-related debris flow initiation, Cerro Grande fire, New Mexico: Hydrological Processes, v. 15, p. 3011–3023.

Cannon, S.H., Gartner, J.E., Wilson, R.C., Bowers, J.C., and Laber, J.L., 2008, Storm rainfall conditions for floods and debris flows from recently burned areas in southwestern Colorado and southern California: Geomorphology, v. 96, p. 250–269.

Cerdà, A., and Doerr, S.H., 2008, The effect of ash and needle cover on surface runoff and erosion in the immediate post-fire period: Catena, v. 74, p. 256–263.

Certini, G., 2005, Effect of fire on properties of forest soils: a review: Oecologia, v. 143, p. 1–10.

Chorover, J., Vitousek, P.M., Everson, D.A., Esperanza, A.M., and Turner, D., 1994, Solution chemistry profiles of mixed-conifer forests before and after fire: Biogeochemistry, v. 26, p. 115–144.

D'Haen, K., Verstraeten, G., and Degryse, P., 2012, Fingerprinting historical fluvial sediment fluxes: Progress in Physical Geography, v. 36, p. 154–186.

DeBano, L.F., 2000, The role of fire and soil heating on water repellency in wildland environments: a review: Journal of Hydrology, v. 231–232, p. 195–206.

Dyrness, C.T., Van Cleve, K., and Levison, J.D, 1989, The effect of wildfire on soil chemistry in four forest types in interior Alaska: Canadian Journal of Forest Research, v. 19, p. 1389–1396.

Ebel, B.A., Moody, J.A., and Martin, D.A., 2012, Hydrologic conditions controlling runoff generation immediately after wildfire: Water Resources Research, v. 48, W03529.

Elliot, J.G., and Parker, R.S., 2001, Developing a post-fire flood chronolgy and recurrence probability from alluvial stratigraphy in the Buffalo Creek watershed, Colorado, USA: Hydrological Processes, v. 15, p. 3039–3051.

Gabet, E.J., and Bookter, A., 2011, Physical, chemical and hydrological properties of Ponderosa pine ash: International Journal of Wildland Fire, v. 20, p. 443–452.

Gabet, E.J., and Sternberg, P., 2008, The effects of vegetative ash on infiltration capacity, sediment transport, and the generation of progressively bulked debris flows: Geomorphology, v. 101, p. 666–673.

Gonzalez Parra, J., Rivero, V.C., and Lopez, I., 1996, Forms of Mn in soils affected by a forest fire: The Science of the Total Environment, v. 181, p. 231–236.

Graham, R., Finney, M., McHugh, C., Cohen, J., Stratton, R., Bradshaw, L., Nikolov, N., and Calkin, D., 2012, Fourmile Canyon Fire Findings: USDA Forest Service, General Technical Report RMRS-GTR-289, 110 p.

Healy, J. "Thin Snowpack in West Signals Summer of Drought." The New York Times, 22 Feb. 2013, accessed online.

Hershfield, D.M., 1961, Rainfall frequency atlas of the United States for durations from 30 minutes to 24 hours and return periods from 1 to 100 years: U.S. Department of Commerce, Technical Paper No. 40, 107 p.

High Plains Regional Climate Center, 2012, Boulder, Colorado (050848) Climate Summary: http://www.hprcc.unl.edu/cgi-bin/cli_perl_lib/cliMAIN.pl?co0848 (accessed Feb. 2012).

Huffman, E.L., MacDonald, L.H., and Stednick, J.D., 2001, Strength and persistence of fire-induced soil hydrophobicity under ponderosa and lodgepole pine, Colorado Front Range: Hydrological Processes, v. 15, p. 2877–2892.

Ice, G.C., Neary, D.G., and Adams, P.W., 2004, Effects of wildfire on soils and watershed processes: Journal of Forestry, p. 16–20.

Johansen, M.P., Hakonson, T.E., Whicker, F.W., and Breshears, D.D., 2003, Pulsed Redistribution of a Contaminant Following Forest Fire: Cesium-137 in Runoff: Journal of Environmental Quality, v. 32, p. 2150–2157.

Kaufmann, M.R., Huckaby, L., and Gleason, P., 2000, Ponderosa pine in the Colorado Front range: long historical fire and tree recruitment intervals and a case for landscape heterogeneity, *in* Proceedings, The Joint Fire Science Conference Workshop, Boise: Idaho, 8 p.

Kim, J.G., Ko, K.-S., Kim, T.H., Lee, G.H., Song, Y., Chon, C.-M., and Lee, J.-S., 2007, Effect of mining and geology on the chemistry of stream water and sediment in a small watershed: Geosciences Journal, v. 11, p. 175–183.

Kirchner, J.W., Finkel, R.C., Riebe, C.S., Granger, D.E., Clayton, J.L., King, J.G., and Megahan, W.F., 2001, Mountain erosion over 10 yr, 10 k.y., and 10 m.y. time scales: Geology, v. 29, p. 591–594.

Kunze, M.D., and Stednick, J.D., 2006, Streamflow and suspended sediment yield following the 2000 Bobcat fire, Colorado: Hydrological Processes, v. 20, p. 1661–1681.

Larsen, I.J., MacDonald, L.H., Brown, E., Rough, D., Welsh, M.J., Pietraszek, J.H., Libohova, Z., Benavides-Solorio, J.D., and Schaffrath, K., 2009, Causes of Post-Fire Runoff and Erosion: Water Repellency, Cover, or Soil Sealing?: Soil Science Society of America Journal, v. 73, p. 1393–1407.

Legleiter, C.J., Lawrence, R.L., Fonstad, M.A., Marcus, W.A., and Aspinall, R., 2003, Fluvial response a decade after wildfire in the northern Yellowstone ecosystem: a spatially explicit analysis: Geomorphology, v. 54, p. 119–136.

Lovering, T.S., and Goddard, E.N., 1950, Geology and ore deposits of the Front Range, Colorado: U.S. Geological Survey, Professional Paper No. 223, 319 p.

MacDonald, L.H., and Stednick, J.D., 2003, Forests and Water: A state-of-the-art review for Colorado: Colorado Water Resources Research Institute, Completion Report No. 196, 65 p.

Marcus, W.A., Meyer, G.A., and Nimmo, D.R., 2001, Geomorphic control of persistent mine impacts in a Yellowstone Park stream and implications for the recovery of fluvial systems: Geology, v. 29, p. 355–358.

Mast, M.A., and Clow, D.W., 2008, Effects of 2003 wildfires on stream chemistry in Glacier National Park, Montana: Hydrological Processes, v. 22, p. 5013–5023.

MesoWest, 2012, University of Utah: http://mesowest.utah.edu (rainfall data for Colorado weather station BTAC2 accessed Sept. 2012).

Meyer, G.A., and Pierce, J.L., 2003, Climatic controls on fire-induced sediment pulses in Yellowstone National Park and central Idaho: a long-term perspective: Forest Ecology and Management, v. 178, p. 89–104.

Meyer, G.A., and Wells, S.G., 1997, Fire-Related Sedimentation Events on Alluvial Fans, Yellowstone National Park, U.S.A: Journal of Sedimentary Research, v. 67, p. 776–791.

Miller, J.F., Frederick, R.H., and Tracey, R.J., 1973, Precipitation-frequency atlas of the western United States, Colorado: National Oceanic and Atmospheric Administration Atlas 2, v. 3, National Weather Service, 67 p.

Moody, J.A., and Martin, D.A., 2001a, Initial hydrologic and geomorphic response following a wildfire in the Colorado Front Range: Earth Surface Processes and Landforms, v. 26, p. 1049–1070.

Moody, J.A., and Martin, D.A., 2001b, Post-fire, rainfall intensity–peak discharge relations for three mountainous watersheds in the western USA: Hydrological Processes, v. 15, p. 2981–2993.

Moody, J.A., Martin, D.A., Haire, S.L., and Kinner, D.A., 2008, Linking runoff response to burn severity after a wildfire: Hydrological Processes, v. 22, p. 2063–2074.

Moody, J.A., Kinner, D.A., and Ubeda, X., 2009, Linking hydraulic properties of fire-affected soils to infiltration and water repellency: Journal of Hydrology, v. 379, p. 291–303.

Moody, J.A., and Martin, D.A., 2009, Synthesis of sediment yields after wildland fire in different rainfall regimes in the western United States: International Journal of Wildland Fire, v. 18, p. 96–115.

Moody, J.A., 2011, An Analytical Method for Predicting Postwildfire Peak
Discharges: U.S. Geological Survey, Scientific Investigations Report No.
5236, 48 p.

Moody, J.A., and Ebel, B.A., 2012, Hyper-dry conditions provide new insights into
the cause of extreme floods after wildfire: Catena, v. 93, p. 58–63.

Murphy, S.F., Verplanck, P.L., and Barber, L.B., editors, 2000, Comprehensive water
quality of the Boulder Creek Watershed, Colorado, under high-flow and low-flow
conditions: U.S. Geological Survey, Water-Resources Investigations Report 03–
4045, 198 p.

Murphy, S.F., Writer, J.H., and McCleskey, R.B., 2012, Effects of flow regime on
stream turbidity and suspended solids after wildfire, Colorado Front Range, *in*
Proceedings, Wildfire and Water Quality: Processes, Impacts and Challenges,
Banff, Canada, June 2012, IAHS Publ. 354, 8 p.

National Atmospheric Deposition Program, 2012, Monitoring Location CO94:
http://nadp.sws.uiuc.edu/sites/siteinfo.asp?net=NTN&id=CO94 (accessed
Sept. 2012).

Onda, Y., Dietrich, W.E., and Booker, F., 2008, Evolution of overland flow after a
severe forest fire, Point Reyes, California: Catena, v. 72, p. 13–20.

Owens, P.N., Blake, W.H., and Petticrew, E.L., 2006, Changes in sediment sources
following wildfire in mountainous terrain: a paired-catchment approach,
British Columbia, Canada: Water, Air, and Soil Pollution, v. 6, p. 273–381.

Parise, M., and Cannon, S.H., 2012, Wildfire impacts on the processes that generate
debris flows in burned watersheds: Natural Hazards, v. 61, p. 217–227.

Pierce, J.L., Meyer, G.A., and Jull, T.A.J., 2004, Fire-induced erosion and millennial-
scale climate change in northern ponderosa pine forests: Nature, v. 432, p. 87–
90.

Plumlee, G.S., Martin, D.A., Hoefen, T., Kokaly, R., Hageman, P., Eckberg, A.,
Meeker, G.P., Adams, M., Anthony, M., and Lamothe, P.J., 2007, Preliminary
analytical results for ash and burned soils from the October 2007 southern
California Wildfires: U.S. Geological Survey, Open-File Report No. 1407, 13
p.

Reneau, S.L., Katzman, D., Kuyumjian, G.A., Lavine, A., and Malmon, D.V., 2007,
Sediment delivery after a wildfire: Geology, v. 35, p. 151–154.

Rhoades, C.C., Entwistle, D., and Butler, D., 2011, The influence of wildfire extent and severity on streamwater chemisty, sediment and temperature following the Hayman Fire, Colorado: International Journal of Wildland Fire, v. 20, p. 430–442.

Ruddy, B.C., Stevens, M.R., Verdin, K.L., and Elliott, J.G., 2010, Probability and volume of potential postwildfire debris flows in the 2010 Fourmile burn area, Boulder County, CO: U.S. Geological Survey, Open-File Report No. 1244: 13 p.

Ryan, S.E., Dwire, K.A., and Dixon, M.K., 2011, Impacts of wildfire on runoff and sediment loads at Little Granite Creek, western Wyoming: Geomorphology, v. 129, p. 113–130.

Saunders, S., Montogmery, C., and Easley, T., 2008, Hotter and drier: The West's changed climate: Rocky Mountain Climate Organization and National Resources Defense Council, 64 p.

Schoennagel, T. "Fourmile Fire Follows Historical Pattern." Interview by Andrea Dukakis. Colorado Matters, Colorado Public Radio, 15 Sept. 2010, accessed online.

Shakesby, R.A., and Doerr, S.H., 2006, Wildfire as a hydrological and geomorphological agent: Earth-Science Reviews, v. 74, p. 269–307.

Sherriff, R.L., and Veblen, T.T., 2007, A spatially-explicit reconstruction of historical fire occurrence in the ponderosa pine zone of the Colorado Front Range: Ecosystems, v. 10, p. 311–323.

Smith, H.G., Sheridan, G.J., Lane, P.N.J., Nyman, P., and Haydon, S., 2011a, Wildfire effects on water quality in forest catchments: A review with implications for water supply: Journal of Hydrology, v. 396, p. 170–192.

Smith, H.G., Sheridan, G.J., Lane, P.N.J., Noske, P.J., and Heijnis, H., 2011b, Changes to sediment sources following wildfire in a forested upland catchment, southeastern Australia: Hydrological Processes, v. 25, p. 2878–2889.

Smith, H.G., Blake, W.H., and Owens, P.N., 2012, Discriminating fine sediment sources and the application of sediment tracers in burned catchments: a review: Hydrological Processes, published online, accessed Oct. 2012.

Soto, B., Basanta, R., and Diaz-Fierros, F., 1993, Influence of wildland fire on surface runoff from a hillslope: Acta Geologica Hispanica, v. 28, p. 95–102.

Stoof, C.R., Wesseling, J.G., and Ritsema, C.J., 2010, Effects of fire and ash on soil water retention: Geoderma, v. 159, p. 276–285.

Sullivan, A.B., and Drever, J.I., 2001, Spatiotemporal variability in stream chemistry in a high-elevation catchment affected by mine drainage: Journal of Hydrology, v. 252, p. 237–250.

Swanson, F.J., 1981, Fire and geomorphic processes in Mooney, H.A., Bonnicksen, T.M., Christensen, N.L., Lotan, J.E., and Reiners, W.A., editors, Proceedings of the conference on fire regimes and ecosystem properties, USDA Forest Service General Technical Report WO v. 26, p. 401–421.

Trimble, S.W., 2009, Fluvial processes, morphology and sediment budgets in the Coon Creek Basin, WI, USA, 1975–1993: Geomorphology, v. 108, p. 8–23.

Twitty, E., 2007, Amendment to Metal Mining and Tourist Era Resources of Boulder County Multiple Property Listing: National Park Service, National Register of Historic Places, NPS Form 10-900-b, OMB No. 1024-0018, 416 p.

Urban Drainage and Flood Control District, 2012, OneRain weather data: http://udfcd.onerain.com/home.php (rainfall data for Colorado stations 4110, 4130, 4140, 4150, and 4730 accessed Sept. 2012).

U.S. Geological Survey, 2012, StreamStats Colorado: http://streamstats.usgs.gov/colorado.html (accessed Nov. 2012).

U.S. Geological Survey, 2012, Surface-Water Data for the Nation: http://nwis.waterdata.usgs.gov/nwis/sw (streamflow data for Colorado gauging stations 06727500 and 06727410 accessed Jul.–Oct. 2012).

Westerling, A.L., Hidalgo, H.G., Cayan, D.R., and Swetnam, T.W., 2006, Warming and earlier spring increase western U.S. forest wildfire activity: Science, v. 313, p. 940–943.

Wilkinson, S.N., Wallbrink, P.J., Hancock, G.J., Blake, W.H., Shakesby, R.A., and Doerr, S.H., 2009, Fallout radionuclide tracers identify a switch in sediment sources and transport-limited sediment yield following wildfire in a eucalypt forest: Geomorphology, v. 110, p. 140–151.

Wondzell, S.M., and King, J.G., 2003, Postfire erosional processes in the Pacific Northwest and Rocky Mountain regions: Forest Ecology and Management, v. 178, p. 75–87.

Woods, S.W., and Balfour, V.N., 2010, The effects of soil texture and ash thickness on the post-fire hydrological response from ash-covered soils: Journal of Hydrology, v. 393, p. 274–286.

Writer, J.H., McCleskey, R.B., and Murphy, S.F., 2012, Effects of wildfire on source-water quality and aquatic ecosystems, Colorado Front Range, *in* Proceedings, Wildfire and Water Quality: Processes, Impacts and Challenges, Banff, Canada, June 2012, IAHS Publ. 354, 6 p.

Writer, J.H., and Murphy, S.F., 2012, Wildfire Effects on Source-Water Quality–Lessons from Fourmile Canyon Fire, Colorado, and Implications for Drinking-Water Treatment: U.S. Geological Survey, Fact Sheet No. 3095, 4 p.